ESD-TR-68-157, Vol. II

MODELS FOR ANALYSIS OF THE CAPABILITIES OF GROUND BASED SENSORS IN DETERMINING THE MASS OF ORBITING BODIES - Extended Models

August 1967

SPACE DEFENSE SYSTEMS PROGRAM OFFICE
ELECTRONIC SYSTEMS DIVISION
AIR FORCE SYSTEMS COMMAND
UNITED STATES AIR FORCE
L. G. Hanscom Field, Bedford, Massachusetts

(Prepared under Contract No. F19628-67-C0041 by Westinghouse Defense and Space Center, Surface Division, Baltimore, Maryland)

LEGAL NOTICE

When U. S. Government drawings, specifications or other data are used for any purpose other than a definitely related government procurement operation, the government thereby incurs no responsibility nor any obligation whatsoever; and the fact that the government may have formulated, furnished, or in any way supplied the said drawings, specifications, or other data is not to be regarded by implication or otherwise as in any manner licensing the holder or any other person or conveying any rights or permission to manufacture, use, or sell any patented invention that may in any way be related thereto.

OTHER NOTICES

Do not return this copy. Retain or destroy.

ESD-TR-68-157, Vol. II

MODELS FOR ANALYSIS OF THE CAPABILITIES OF GROUND BASED SENSORS IN DETERMINING THE MASS OF ORBITING BODIES - Extended Models

August 1967

SPACE DEFENSE SYSTEMS PROGRAM OFFICE
ELECTRONIC SYSTEMS DIVISION
AIR FORCE SYSTEMS COMMAND
UNITED STATES AIR FORCE
L. G. Hanscom Field, Bedford, Massachusetts

(Prepared under Contract No. F19628-67-C0041 by Westinghouse Defense and Space Center, Surface Division, Baltimore, Maryland)

FOREWORD

This report is submitted by the Surface Division, Westinghouse Defense and Space Center, Baltimore, Maryland to the Space Defense Systems Program Office, Electronics Systems Division, U.S. Air Force Systems Command, L.G. Hanscom Field, Bedford, Massachusetts. It covers work performed under Task II, Part 1 of Contract F19628-67-C0041 over the period 13 September 1966 to 24 April 1967. It is Technical Report Number 3 of six required technical reports.

A. AVAILABILITY

U. S. Government agencies may obtain copies of this report directly from the Defense Documentation Center. Other qualified DDC users will request through Headquarters (ESTI), Electronics Systems Division, U.S. Air Force Systems Command, L.G. Hanscom Field, Bedford, Massachusetts.

B. REPRODUCTION

This report may be reproduced to satisfy needs of U. S. Government Agencies. No other reproduction is authorized except with permission of Headquarters (ESTI), Electronics Systems Division, U.S. Air Force Systems Command, L.G. Hanscom Field, Bedford, Massachusetts.

C. LEGAL NOTICE

When U. S. Government drawings, specifications, or other data are used for any purpose other than a definitely related Government procurement operation, the Government incurs no responsibility nor any obligation whatsoever, and the fact that the Government may have formulated, furnished, or in any way supplied the said drawings, specifications, or other data, is not to be regarded by implication or otherwise, or in any manner licensing the holder or any other person or corporation, or conveying any rights or permission to manufacture, use, or sell any patented invention that may in any way be related thereto.

D. DISPOSITION

Do not return this copy. Retain or destroy.

E. APPROVAL

This technical report has been reviewed and approved 31 July 1967.

Bernard J. Filliatreault
Contracting Officer
Space Defense/Command
Systems Program Office

ABSTRACT

This report contains a description of the models to be used in analyzing the capabilities of ground-based sensors in determining the mass of orbiting bodies, model coefficients, and the justification for their selection. Relations are derived for computing sensitivity coefficients and their coupling to mass variance for the case of noisy, biased sensors (monostatic and tri-static radars, Baker - Nunn cameras), and for spherical and tumbling cylindrical satellites.

TABLE OF CONTENTS

SECTION I

INTRODUCTION

This document is the second in a series of three theoretical reports prepared under Air Force Contract F19628-67-C0041. The first of the series, Technical Report Number 1 of the referenced contract, was concerned with the mathematical models and relationships necessary to perform a detailed maximum-likelihood/minimum-variance error analysis of the capability of ground-based sensors in determining the mass of a satellite[5*]. It was specialized to account for the following restrictions:

1) The sensors observed the satellite without error.

2) The satellite was a sphere of 5-meter diameter.

3) All the physical characteristics of the body except mass were known without error.

4) All the error in the computed mass resulted from errors and uncertainties in the knowledge of the orbit-perturbing forces.

The present report is a companion document, extending the theoretical development to remove the restrictions of perfect sensor observations and of perfect knowledge of the non-mass body characteristics. In addition, the body shapes are generalized from the sphere of the preceding report to include also one of a pair of cylindrical objects of length 10 meters and diameters 2 and 5 meters, respectively. The cylinders are free to tumble in a propellor motion, with the tumble axis perpendicular to the flight path.

Since the analysis in many places depends upon the developments

* Superscript numerals denote entries in the References Section of the present report.

of the previous report[5], it is suggested that the reader have that document available for reference.

SECTION II

PERTURBATIONS TO TWO-BODY MOTION

A. GENERAL EQUATIONS OF MOTION

In general,

$$d\underline{x}/dt = \underline{f}(\underline{x}, t) + \underline{F}(\underline{x}, \underline{\xi}, \underline{u}, t), \tag{2.1}$$

$$d\underline{\xi}/dt = \underline{G}(\underline{x}, \underline{\xi}, \underline{u}, t), \tag{2.2}$$

where

$$\underline{x}(t) = \begin{bmatrix} x_1 \\ x_2 \\ x_3 \\ x_4 \\ x_5 \\ x_6 \end{bmatrix} = \begin{bmatrix} x \\ y \\ z \\ \dot{x} \\ \dot{y} \\ \dot{z} \end{bmatrix}$$

is the state vector describing completely the orbit at any time t, $\underline{f}$ is the vector of two-body accelerations

$$\underline{f}(\underline{x},t) = \begin{bmatrix} x_4 \\ x_5 \\ x_6 \\ -\mu x_1/r^3 \\ -\mu x_2/r^3 \\ -\mu x_3/r^3 \end{bmatrix},$$

and $\underline{F}$ is the vector of non-two-body accelerations

$$\underline{F}(\underline{x}, \underline{\xi}, \underline{u}, t) = \begin{bmatrix} 0 \\ \hline \ddot{\underline{r}}_{drag} \end{bmatrix} + \begin{bmatrix} 0 \\ \hline \ddot{\underline{r}}_{solar} \end{bmatrix} + \begin{bmatrix} 0 \\ \hline \ddot{\underline{r}}_{sun,\ moon} \end{bmatrix} + \begin{bmatrix} 0 \\ \hline \underline{F}_o \end{bmatrix}, \tag{2.3}$$

where

$\ddot{\underline{r}}_{drag}$ = atmospheric drag acceleration vector,

$\ddot{\underline{r}}_{solar}$ = solar pressure acceleration vector,

$\ddot{\underline{r}}_{sun,\ moon}$ = gravitational acceleration vector due to the sun and moon taken as point masses,

$\underline{F}_o$ = gravitational acceleration vector due to the asphericity of the earth

The vector $\underline{\mathcal{E}}$ can be as large as a six-dimensional state vector which describes rigid-body rotation, having the Euler angles of the satellite as its first three elements and their time derivatives as its remaining three. The rotational excitation vector $\underline{G}(\underline{x}, \underline{\mathcal{E}}, \underline{u}, t)$ reflects the possible coupling of the orbit to the rotation, e.g., through gravity-gradient torquing, and the coupling of the dynamic biases, as, for example, drag, to these rotations.

The vector $\underline{\mathcal{E}}$ appears in $\underline{F}$ both because the rotations present changing cross-sectional areas in $\ddot{\underline{r}}_{drag}$ and $\ddot{\underline{r}}_{solar}$, and because of the conservative exchange of energy between the translational motion of the orbit and the rotational motion of the satellite about its center of mass. That is, if the satellite tumble-rate increases in a conservative field, the kinetic energy must come from somewhere, and that "somewhere" is the translational energy of the orbit.

This conservative coupling is investigated in Appendix I of this report, where it is shown that it is indeed possible to de-orbit a satellite in a non-dissipative environment using only torque devices. However, the minimum de-orbiting time is shown to be on the order of 10^6 years, so this conservative coupling of $\underline{\mathcal{E}}$ to $\underline{x}$ can be, and is in (2.3), ignored.

B. TUMBLING MODE

The mode of tumbling for non-spherical satellites is restricted under this contract to be a propellor-like motion, with the axis of rotation directed along the satellite's velocity vector. Since, also, the non-spherical satellites are designated to be cylinders, it is clear that the same cross-sectional area of a satellite is always presented to the atmospheric drag mechanism. As far as $\underline{\ddot{r}}_{drag}$ is concerned, then, it is not a function of the rotations $\underline{\xi}(t)$.

Since the sun and earth see changing aspect areas for this mode of tumbling, the direct and earth-reflected solar pressure vector $\underline{\ddot{r}}_{solar}$ is, however, a function of $\underline{\xi}(t)$.

Two things must now be done: the precise dynamics of $\underline{\xi}(t)$ must be established or assumed, and the functional dependence of $\underline{\ddot{r}}_{solar}$ upon $\underline{\xi}(t)$ must be derived.

1. Rotation Dynamics

In order that the tumbling plane turn with the satellite velocity vector, i.e., in order that the velocity unit vector $\hat{i}_r$ always be normal to the tumble plane, as shown in Figure 1, below, torques internal to the satellite must be assumed. For simplicity, it will be assumed that these interval torques are such that the tumble rate, say $\dot{\xi}$, is a constant relative to the normal $\hat{i}_n$ to the orbital plane. Because of the non-two-body effects, $\hat{i}_n$ will move in inertial space, and so the tumble rate will not be inertially constant. Since the nutation rate of the orbital plane is relatively small, the satellite torques necessary to explain this inertially accelerating motion would also be small. In any event, the motion assumed is as valid as any other once the propellor motion is

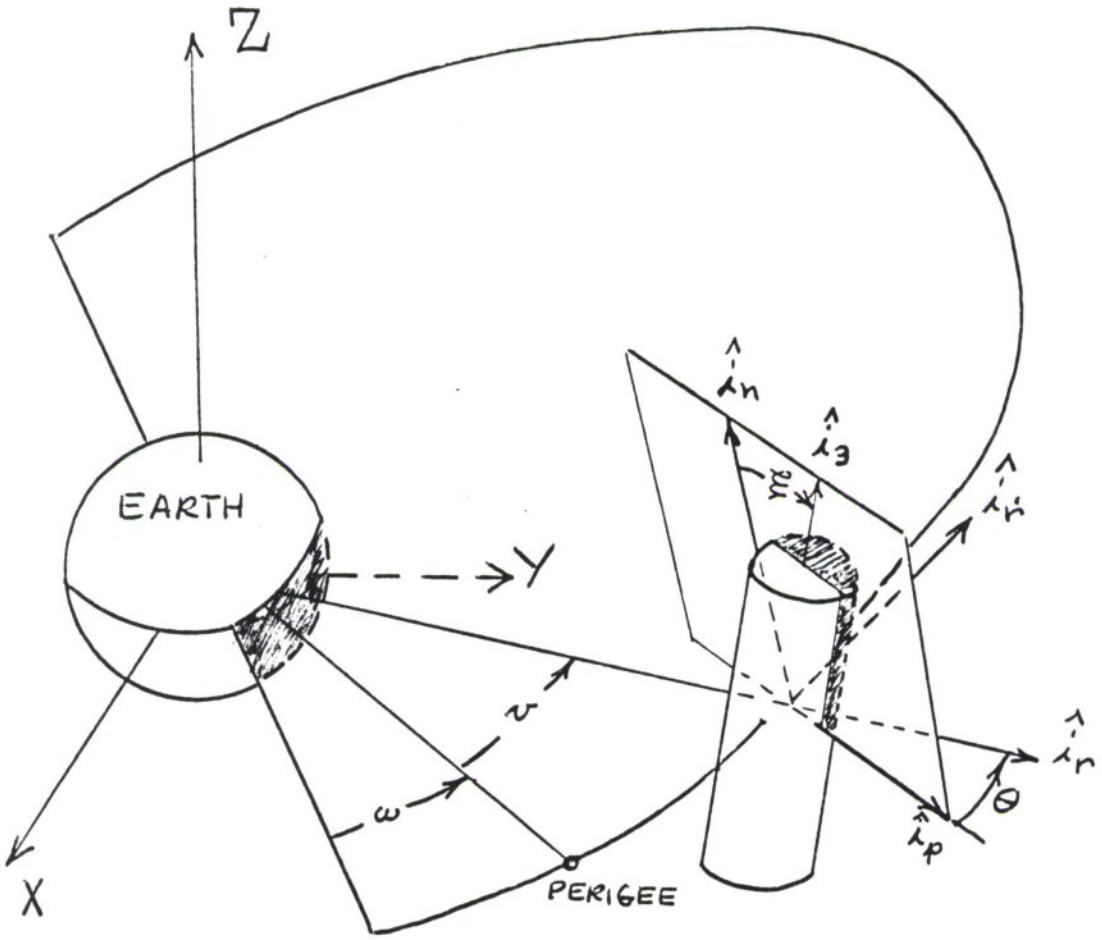

FIGURE 1. TUMBLING GEOMETRY

presumed, and the results of the error analysis will at least be indicative of the importance of accurate signature data.

The tumble model is, in algebraic terms,

$$\underline{\xi}(t) = \underline{\xi}_o + (t-t_o)\dot{\underline{\xi}}\,, \tag{2.4}$$

with the rotation state $\underline{\xi}$ defined as the 2-vector

$$\underline{\xi}\ (t) = \begin{bmatrix} \underline{\xi} \\ \dot{\underline{\xi}} \end{bmatrix} .$$

If the errors in the constants $\underline{\xi}_o$ and $\dot{\underline{\xi}}$ were to be modeled (a covariance matrix for them introduced in the estimation equations), then $\underline{G}$ in (2.2) would have to be explicitly written to express the dynamics of constant-velocity. While this is very simple to do, we will take the errors in $\underline{\xi}_o$ and $\dot{\underline{\xi}}$ to be unmodeled errors and find, by the quasi-experimental means discussed in Section IV.D of Reference 5, the sensitivity coefficients $\partial \underline{v}_1/\partial \underline{\xi}$. This will indicate the relative importance of signature information without depending on the reasonableness of any assumed value for a covariance matrix on $\underline{\xi}$.

2. Solar Pressure as a Function of Tumble

The details of how $\ddot{\underline{r}}_{solar}$ functionally depends on $\underline{\xi}$ are derived in Appendix II of this report. In summary, the results are as follows. Define:

k_r = specular reflectivity of satellite,

k_d = diffuse reflectivity of satellite,

q = Earth albedo,

λ = ratio of earth radius to distance between satellite and earth center,

B_λ = arc cos λ ,

I_s = solar constant,

c = speed of light,

$\hat{i}_r$ = unit vector from center of earth to center of satellite,

$\hat{i}_{\dot{r}}$ = unit velocity vector of satellite

$\hat{i}_{ss}$ = unit vector from center of sun to earth,

$\cos\alpha = -(\hat{i}_r \cdot \hat{i}_{ss})$,

$$p_1 = \begin{cases} \lambda q (a_1 + a_2) \cos\alpha, & |\alpha| \le \pi/2 - B_\lambda \\ \lambda q a_r, & \pi/2 - B_\lambda \le |\alpha| \le \pi/2 + B_\lambda \\ 0, & \pi/2 + B_\lambda \le |\alpha| \le \pi \end{cases}$$

$$p_2 = \begin{cases} (1 + \lambda q a_2), & |\alpha| \le \pi/2 - B_\lambda \\ (1 + \lambda q a_{ss}), & \pi/2 - B_\lambda \le |\alpha| \le \pi/2 + B_\lambda \\ 0, & \pi/2 + B_\lambda \le |\alpha| \le \pi \end{cases}$$

$a_1 = (-.0417 + .5431\lambda)/3$,

$a_2 = \{.0444 - 3.17(\lambda - .77)^3 + .0045(\lambda - .77)\sin[14.3(\lambda - .77)\pi]\}/3$

$a_{ss} = a_2[1 + s - se^{s\tau y} - e^{-\tau y}(2 + sy)]/2$

$a_r = \{a_{ss} + (a/2)[s + 1 - s(1 + sy)^d]\}\cos\alpha$

$$+\left\{\frac{\lambda^2[(1\lambda - \sin\alpha)^3 + (\lambda - \sin\alpha)^3]}{(1+\lambda^2 - 2\lambda\sin\alpha)^{3/2}} - \frac{(1-\lambda^2)^{3/2}}{\lambda}\right\}\frac{\sin\alpha}{6},$$

$\tau = -4 + 9.3\lambda$

$y = (\alpha - \pi/2)/B_\lambda$

$$s = \begin{cases} 1, & y \le 0, \\ -1, & y > 0, \end{cases}$$

$d = 3.7 + 59(\lambda - .77)^2$,

$\sin\theta = \hat{i}_r \cdot \hat{i}_{\dot{r}}$,

$\cos\theta = \sqrt{1 - \sin^2}$,

$\hat{i}_n = (\hat{i}_r \times \hat{i}_{\dot{r}})/\cos\theta$, the normal to the orbital plane,

$\hat{i}_p = \hat{i}_r \times \hat{i}_n$, the vector normal to $\hat{i}_n$ that defines the tumble plane (see Figure 1),

$$\hat{i}_3 = \sin \xi \, \hat{i}_p + \cos \xi \, \hat{i}_n$$

$$\cos \alpha_s = \hat{i}_{ss} \cdot \hat{i}_3 \ ,$$

$$\cos \alpha_r = \hat{i}_r \cdot \hat{i}_3 \ ,$$

$$\cos \phi = (p_1 \cos \alpha_r + p_2 \cos \alpha_s) / \sqrt{p_1^2 + p_2^2}$$

$A = \pi R_s^2$, the cross-sectional area of a sphere of radius R_s,

$A_b = \pi R_c^2$, the area of the base of a cylirder of radius R_c,

$A_l = 2LR_c$, cross-sectional area normal to the base of a cylinder of length L.

Then the solar radiation acceleration is, for a

Spherical Satellite:

$$\ddot{\underline{r}}_{solar} = (I_s/c)\,(A/m) \left[(1 + 4k_d/9) \, (p_1 \, \hat{i}_r + p_2 \, \hat{i}_{ss}) \right] \ ; \tag{2.5}$$

Cylindrical Satellite:

$$\begin{aligned} \ddot{\underline{r}}_{solar} = (I_s/c)\,(A_l/m) \Big[& \left[(A_b/A_l)\,(1-k_r)\,|\cos\phi| \right. \\ & \left. + \pi k_d/6 + (1 + k_r/3)\,|\sin\phi| \right] \left[p_1 \, \hat{i}_r + p_2 \, \hat{i}_{ss} \right] \\ & + \left[2\,(A_b/A_l)\,(k_r\,|\cos\phi| + k_d/3) - (4/3)k_r\,|\sin\phi| \right. \\ & \left. - \pi k_d/6 \right] \left[\, p_1 \cos\alpha_r + p_2 \cos\alpha_s \, \right] \hat{i}_3 \Big] \end{aligned} \tag{2.6}$$

Taking the "ballistic" coefficient with respect to solar pressure to be

$$u_3 = \begin{cases} (I_{nom}/c)\,(A/m) \ , \text{ spherical case,} \\ (I_{nom}/c)\,(A_l/m) \ , \text{ cylindrical case,} \end{cases} \tag{2.7}$$

where

$$I_s = I_{nom} (R_{es}/r_{es})^2 \quad ,$$

where R_{es} is the mean earth-sun distance and r_{es} is the actual earth-sun distance, it is clear from (2.5) and (2.6) that the $\underline{\gamma}$ vector that represents $\partial \ddot{\underline{r}}_{solar}/\partial u_3$ is simply the terms in (2.5) or (2.6), respectively, enclosed in the large square brackets times $(R_{es}/ r_{es})^2$:

$$\underline{\gamma} = (R_{es}/r_{es})^2 \left[\text{terms in large square brackets in (2.5) or (2.6)}\right] \tag{2.8}$$

SECTION III

ESTIMATION AND PREDICTION

A. PRELIMINARY DETAILS

Consider equations (4.1) and (4.2) from Reference 5, suitably modified to account for the tumbling of a non-spherical satellite:

$$d(\Delta\underline{x})/dt = \underline{f}(\underline{x}, t) - \underline{f}(\underline{x}^o, t) + \underline{F}(\underline{x}, \underline{\xi}, \underline{u}, t), \tag{3.1}$$

$$\Delta\underline{z} = \underline{h}(\underline{x}, \underline{\eta}, \underline{b}, t) - \underline{h}(\underline{x}^o, 0, 0, t), \tag{3.2}$$

where $\Delta\underline{x}(t)$ is the Encke variation from the two-body orbit $\underline{x}^o(t)$ to the actual orbit $\underline{x}(t)$, $\underline{f}$ is the vector of two-body accelerations, and $\underline{F}$ is the vector of non-two-body accelerations,

$$\underline{F}(\underline{x}, \underline{\xi}, \underline{u}, t) = \begin{bmatrix} 0 \\ \hline \underline{F}_{drag} \end{bmatrix} + \begin{bmatrix} 0 \\ \hline \underline{F}_{solar} \end{bmatrix} + \begin{bmatrix} 0 \\ \hline \underline{F}_{sun,\ moon} \end{bmatrix} + \begin{bmatrix} 0 \\ \hline \underline{F}_{o} \end{bmatrix}$$

developed in detail in that reference and in Section II of this report.

The vector $\underline{u}$ contained in $\underline{F}$ represents the dynamic biases affecting the satellite. The first three of its components,

$$\underline{v}_1(t) = \begin{bmatrix} u_1 \\ u_2 \\ u_3 \end{bmatrix},$$

are "ballistic" coefficients which will be actively estimated. The remaining three of its components account for uncertainties in the oblateness forces $\underline{F}_o$ due to errors in $\underline{x}$ and in the geopotential coefficients $\underline{J}$. These are defined by the 3-vector

$$\underline{v}_2(t) = \underline{F}_o(\underline{x}, \underline{J}) - \underline{F}_o(\hat{\underline{x}}, \hat{\underline{J}}),$$

where $\underline{x} = \hat{\underline{x}}(t\ /t_{n-1})$ and $\hat{\underline{J}}$ are the best estimates of $\underline{x}(t)$ and $\underline{J}$ at time t given all data upto and including time t_{n-1}. To first-order accuracy,

$$\underline{v}_2(t) = \left(\frac{\hat{\partial \underline{F}_o}}{\partial \underline{r}}\right)\left[\Delta\underline{r}(t) - \Delta\hat{\underline{r}}(t/t_{n-1})\right] + \left(\frac{\hat{\partial \underline{F}_o}}{\partial \underline{J}}\right)\Delta\underline{J}, \qquad (3.3)$$

where $\underline{r}$ and $\Delta\underline{r}$ are the first three components (the position components) of $\underline{x}$ and $\Delta\underline{x}$, respectively. The hats over the partial derivatives indicate that they are evaluated around $\hat{\underline{r}}(t\ /t_{n-1})$ and $\hat{\underline{u}}(t/t_{n-1})$.

The 2-vector $\underline{\xi}(t)$ contained in $\underline{F}$ describes the rotations of the cylindrical satellites to be considered in this phase of the study. Since there are no very obvious covariance matrices applicable to $\underline{\xi}(t)$, it will be treated as an unmodeled parameter. In keeping with the discussion on sensitivity coefficients in Section IV.D of Reference 5, the study will therefore seek the sensitivity matrix $\partial\underline{u}/\partial\underline{\xi}$ in order to ascertain the importance of errors in our knowledge of tumble position and rate. A detailed analysis of the tumbling mode called out in this study is performed in Section II of the present report.

In (3.2),

$$\underline{z} = \underline{h}(\underline{x},\ \underline{\eta}\ ,\ \underline{b}\ ,\ t) \qquad (3.4)$$

defines the observations $\underline{z}(t)$ on the orbit, where

$\underline{\eta}(t)$ = zero-mean Gaussian white noise,

$\underline{b}$ = constant but unknown biases,

$\Delta\underline{z}(t) = \underline{z} - \underline{z}^o$, the difference between the actual noisy observation and the noise-free observation of the two-body part of the motion.

Now, we can define the error vector

$\underline{e}_a\,(t/t_k) = \underline{a}\,(t) - \hat{\underline{a}}\,(t/t_k)$ for any vector $\underline{a}\,(t)$. In the special cases where t assumes discrete values t_n, the notation will be simplified to $\underline{e}_a\,(n/k)$.

With the q-vector $\underline{y}(t)$ defined as the column of variables which are to be actively estimated, i.e.,

$$\underline{y}(t) = \begin{bmatrix} \Delta\underline{x} \\ \hline \underline{v}_1 \end{bmatrix} , \tag{3.5}$$

the difference equation relating the one-step prediction errors to the prior in-step estimation errors is (equation (4.31), Reference 5)

$$\underline{e}_y(n/n-1) = \Phi_y(n, n-1)\,\underline{e}_y(n-1/n-1) + \frac{\partial \underline{y}}{\partial \underline{v}_2}(n, n-1)\,\underline{e}_{v_2}(n-1/n-1) + \underline{\omega}(n-1), \tag{3.6}$$

where

$$\Phi_y(n, n-1) = \left[\begin{array}{c|c} \Phi(n, n-1) & \frac{\partial \underline{x}}{\partial \underline{v}_1}(n, n-1) \\ \hline 0 & \begin{matrix} e^{-T_n/\tau_d} & & \\ & 1 & \\ & & 1 \end{matrix} \end{array}\right],$$

$T_n = t_n - t_{n-1}$,

$\Phi\,(n,n-1)$ = the two-body transition matrix for the states $\underline{x}$ (see Appendix IV, Reference 5),

$$\frac{\partial \underline{x}}{\partial \underline{v}_1}(t, s) = \int_s^t \Phi(t, \alpha) \left[\begin{array}{c|c|c} 0 & 0 & 0 \\ \hline \hat{\underline{\beta}}(\alpha)e^{-(\alpha-s)/\tau_d} & \hat{\underline{\beta}}(\alpha) & \hat{\underline{\gamma}}(\alpha) \end{array}\right] d\alpha,$$

$\hat{\beta}(\alpha)$, $\hat{\underline{\gamma}}(\alpha) = \partial \ddot{\underline{r}}_{drag} / \partial u_1$ and $\partial \ddot{\underline{r}}_{solar} / \partial u_3$ evaluated around the best state estimate $\hat{\underline{x}}(t/s)$,

$$\frac{\partial \underline{y}}{\partial \underline{v}_2}(n, n-1) = \int_{t_{n-1}}^{t_n} \Phi_y(t_n, s)\, ds \begin{bmatrix} 0 & 0 & 0 \\ 0 & 0 & 0 \\ 0 & 0 & 0 \\ 1 & 0 & 0 \\ 0 & 1 & 0 \\ 0 & 0 & 1 \\ 0 & 0 & 0 \\ 0 & 0 & 0 \\ 0 & 0 & 0 \end{bmatrix}, \qquad \underline{\omega}(n-1) = \int_{t_{n-1}}^{t_n} \Phi_y(t_n, s) \begin{bmatrix} 0 \\ \vdots \\ 0 \\ \hline w_1(s) \\ 0 \\ 0 \end{bmatrix} ds,$$

$w_1(t)$ = zero-mean Gaussian white noise with power $(2/\tau_d)\, \sigma^2_{drag}$ per unit double bandwidth in rad./sec.

Finally the following definitions for covariance matrices will be needed.

For any vectors $\underline{a}(t)$ and $\underline{b}(t)$,

$$\text{Cov}\left[\underline{a}(t), \underline{b}(t)\right] = E\left[\underline{a}(t)\, \underline{b}^T(t)\right] - E\left[\underline{a}(t)\right] E\left[\underline{b}^T(t)\right],$$

where $E(\ )$ denotes mathematical expectation and $(\ )^T$ denotes matrix transpose,

$$\text{Cov}\left[\underline{a}(t), \underline{a}(t)\right] = \text{Cov}\ \underline{a}(t)$$

and

$$P_{ab}(n/k) = \text{Cov}\left[\underline{a}(n) - \hat{\underline{a}}(n/k), \underline{b}(n) - \hat{\underline{b}}(n/k)\right] = \text{Cov}\left[\underline{e}_a(n/k), \underline{e}_b(n/k)\right]$$

The covariances on the environment are

$$Q_{yy}(n) = \text{Cov}\ \underline{\omega}(n),$$

$$R_{\eta\eta}(n) = \text{Cov}\ \underline{\eta}(n),$$

$$R_{bb} = \text{Cov}\ \underline{b},$$

with

$$\text{Cov}\left[\underline{\omega}(n), \underline{\omega}(m)\right] = \text{Cov}\left[\underline{\eta}(n), \underline{\eta}(m)\right] = 0, \; m \neq n,$$

and all cross-variances among $\underline{\omega}$, $\underline{\eta}$, and $\underline{b}$ identically zero.

B. MINIMUM-VARIANCE DERIVATION

1. Fundamental Expressions

The derivations depend upon three basic expressions: the one-step prediction error equation already presented as (3.6), a linearized observation equation developed from (3.2), and the in-step estimation equation which develops from the linear regression solution to the minimum-variance problem.

The linear regression solution is characterized as

$$\hat{\underline{y}}(n/n) = \hat{\underline{y}}(n/n-1) + B_y(n)\left[\Delta\underline{z}(n) - \Delta\hat{\underline{z}}(n/n-1)\right] \tag{3.7}$$

where $B_y(n)$ is a gain matrix to be determined and where, from (3.2),

$$\Delta\underline{z}(n) - \Delta\hat{\underline{z}}(n/n-1) = \underline{h}\left[\underline{x}, \underline{\eta}, \underline{b}, t\right] - \underline{h}\left[\underline{x}^{\circ}, 0, 0, t\right] - \underline{h}\left[\underline{x}(n/n-1), 0, 0, t\right] + \underline{h}\left[\underline{x}^{\circ}, 0, 0, t\right]. \tag{3.8}$$

After a first-order expansion around $\hat{\underline{x}}(n/n-1)$, the latter can be written as

$$\Delta\underline{z}(n) - \Delta\hat{\underline{z}}(n/n-1) = H_y(n)\left[\underline{y}(n) - \hat{\underline{y}}(n/n-1)\right] + H_\eta(n)\underline{\eta}(n) + H_b(n)\underline{b} \tag{3.9}$$

where $$H_y(n) = \left[\begin{array}{c|ccc} H(n) & 0 & 0 & 0 \\ & \vdots & \vdots & \vdots \\ & 0 & 0 & 0 \end{array}\right],$$

$$H(n) = \left.\frac{\partial \underline{h}}{\partial \underline{x}}\right|_{\underline{x} = \hat{\underline{x}}(n/n-1)},$$

$$H_\eta(n) = \left.\frac{\partial \underline{h}}{\partial \underline{\eta}}\right|_{\underline{x} = \hat{\underline{x}}(n/n-1)}$$

$$H_b(n) = \left.\frac{\partial \underline{h}}{\partial \underline{b}}\right|_{\underline{x} = \hat{\underline{x}}(n/n-1)}$$

Subtracting $\underline{y}(n)$ from both sides of (3.7) and employing (3.9), we find

$$\underline{e}_y(n/n) = \left[I - B_y(n)H_y(n)\right]\ \underline{e}_y(n/n-1) - B_y(n)H_\eta(n)\ \underline{\eta}(n) - B_y(n)H_b(n)\underline{b}. \tag{3.10}$$

2. Computation of Optimal Gain $B_y(n)$

As discussed in Reference 5, the minimum-variance gain matrix is found by setting

$$\text{trace}\left\{A\, P_{yy}\,(n/n)\, A\right\} = \min. \tag{3.11}$$

No matter what the form of the weighting matrix A (in Reference 5 we happened to assume it diagonal), the minimum estimation variance obtains from the solution to

$$dP_{yy}\,(n/n) = 0.$$

Since, from (3.10),

$$P_{yy}(n/n) = \left[I-B_yH_y\right] P_{yy}(n/n-1)\, \left[I-B_yH_y\right]^T + B_yH_\eta R_{\eta\eta}(n)\, H_\eta{}^T B_y{}^T$$

$$+ B_yH_bR_{bb}H_b{}^TB_y{}^T - \left[I-B_yH_y\right]P_{yb}(n/n-1)H_b{}^T\, B_y{}^T - B_yH_bP_y{}^T{}_b(n/n-1)\left[I-B_yH_y\right]^T, \tag{3.12}$$

where B_y and the H's have argument (n), it can be shown in the manner of Reference 5 that the optimal gain is

$$B_y(n) = \left[P_{yy}(n/n-1)H_y{}^T(n) + P_{yb}(n/n-1)H_b{}^T(n)\right]\left[H_y(n)P_{yy}(n/n-1)H_y{}^T(n)\right.$$
$$+ H_\eta\,(n)R_{\eta\eta}\,(n)H_\eta{}^T(n) + H_b(n)R_{bb}H_b{}^T(n)$$
$$\left. + H_y(n)P_{yb}(n/n-1)H_b{}^T(n) + H_b(n)P_{yb}^T(n/n-1)H_y{}^T(n)\right]^{-1}. \tag{3.13}$$

Note the covariance matrix $P_{yb}(n/n-1)$ that appears here. If, as in the perfect sensor case, we are to generate the estimation covariances recursively, two new expressions must be derived in addition to those that were needed for perfect sensors: $P_{yb}(n/n-1)$ as a function of $P_{yb}(n-1/n-1)$, and $P_{yb}(n-1/n-1)$ as a function of $B_y(n-1)$ and $P_{yb}(n-1/n-2)$.

3. Prediction Covariance Computations

Directly from the perfect sensor case [5],

$$P_{yy}(n/n-1) = \Phi_y(n, n-1)P_{yy}(n-1/n-1)\Phi_y^T(n, n-1)$$
$$+ \Phi_y(n, n-1)P_{yv_2}(n-1/n-1)\frac{\partial \underline{y}}{\partial \underline{v}_2}^T(n, n-1)$$
$$+ \frac{\partial \underline{y}}{\partial \underline{v}_2}(n, n-1)P_{yv_2}^T(n-1/n-1)\Phi_y^T(n, n-1)$$
$$+ \frac{\partial \underline{y}}{\partial \underline{v}_2}(n, n-1)P_{v_2v_2}(n-1/n-1)\frac{\partial \underline{y}}{\partial \underline{v}_2}^T(n, n-1) + Q_{yy}(n-1), \quad (3.13)$$

$$P_{yJ}(n/n-1) = \left[\Phi_y(n, n-1) + \frac{\partial \underline{y}}{\partial \underline{v}_2}(n, n-1)\frac{\hat{\partial \underline{F}_o}}{\partial \underline{y}}(n-1)\right]P_{yJ}(n-1/n-1)$$
$$+ \frac{\partial \underline{y}}{\partial \underline{v}_2}(n, n-1)\frac{\hat{\partial \underline{F}_o}}{\partial \underline{J}}(n-1)\,P_{JJ}, \quad (3.14)$$

where $P_{JJ} = \mathrm{Cov}(\Delta \underline{J})$, the covariance of the geopotential coefficient errors.

Multiplying (3.6) by $\underline{b}^T$ and taking the expected value, we compute the additional prediction covariance needed for this real sensor case:

$$P_{yb}(n/n\text{-}1) = \left[\Phi_y(n,n\text{-}1) + \frac{\partial \underline{y}}{\partial \underline{v}_2}(n,n\text{-}1) \frac{\partial \hat{\underline{F}}_o}{\partial \underline{y}}(n\text{-}1) \right] P_{yb}(n\text{-}1/n\text{-}1). \tag{3.15}$$

4. In-Step Covariance Computations

Upon substituting the optimal gain $B_y(n)$ defined by (3.13) into equation (3.12), we can rearrange terms and make the appropriate cancellations to obtain

$$P_{yy}(n/n) = \left[I - B_y(n)\, H_y(n)\right] P_{yy}(n/n\text{-}1) - B_y(n)\, H_b(n)\, P_y{}^T{}_b(n/n\text{-}1) \tag{3.16}$$

This is to be compared to (4.41) in Reference 5.

We can post-multiply (3.10) by $\underline{e}_{v_2}^T(n/n) = \underline{v}_2{}^T(n)$, use the definition for $\underline{v}_2(n)$ provided by (3.3), and take the expectation:

$$P_{yv_2}(n/n) = \left[I - B_y(n)\, H_y(n)\right] \left[P_{yy}(n/n\text{-}1) \frac{\partial \hat{\underline{F}}_o}{\partial \underline{y}}{}^T(n) + P_{yJ}(n/n\text{-}1) \frac{\partial \hat{\underline{F}}_o}{\partial \underline{J}}{}^T(n) \right] - B_y(n)\, H_b(n)\, P_y{}^T{}_b(n/n\text{-}1) \frac{\partial \hat{\underline{F}}_o}{\partial \underline{y}}{}^T(n) \tag{3.17}$$

where the argument (n) on the partial derivatives indicates evaluation at the point $\hat{\underline{x}}(n/n)$, and

$$\frac{\partial \underline{F}_o}{\partial \underline{y}} = \left[\begin{array}{c|c|c} \frac{\partial \underline{F}_o}{\partial \underline{r}} & \begin{matrix}0&0&0\\0&0&0\\0&0&0\end{matrix} & \begin{matrix}0&0&0\\0&0&0\\0&0&0\end{matrix} \end{array}\right] .$$

Equation (3.17) is to be compared with (4.42) of Reference 5.

The matrix $P_{v_2v_2}(n/n)$ does not differ from its perfect-sensor form:

$$P_{v_2 v_2}(n/n) = \frac{\hat{\partial \underline{F}_o}}{\partial \underline{r}}(n) P_{rr}(n/n) \frac{\hat{\partial \underline{F}_o}^T}{\partial \underline{r}}(n)$$

$$+ \frac{\hat{\partial \underline{F}_o}}{\partial \underline{J}}(n) P_{JJ} \frac{\hat{\partial \underline{F}_o}^T}{\partial \underline{J}}(n) + \Pi(n/n) + \Pi^T(n/n),$$

where

$$\Pi(n/n) = \frac{\hat{\partial \underline{F}_o}}{\partial \underline{r}}(n)\ P_{rJ}(n/n) \frac{\hat{\partial \underline{F}_o}^T}{\partial \underline{J}}(n). \tag{3.18}$$

However, a new matrix need be computed for the right side of (3.15). Post-multiplying (3.10) by $\underline{b}^T$, we can calculate

$$P_{yb}(n/n) = \left[I - B_y(n)\, H_y(n)\right]\ P_{yb}(n/n-1) - B_y(n)\, H_b(n)\, R_{bb} \tag{3.19}$$

to complete the error-analysis recursions.

The filtering process is the same as in the perfect-sensor case, except that the P_{yb} matrix recursions are new and the microscopic details of the other recursion relationships reflect the observation-noise and bias statistics.

SECTION IV

SENSOR MODELS

Three basic sensor types are to be studied under the subject contract for their performance in mass determination. These are (1) monostatic radars, with observation vector

$$\underline{z}(t) = \begin{bmatrix} \text{Range} \\ \text{Range-Rate} \\ \text{Azimuth} \\ \text{Elevation} \end{bmatrix} = \underline{h}(\underline{x}, \underline{\eta}, \underline{b}, t),$$

(2) tristatic radars, with observation vector

$$\underline{z}(t) = \begin{bmatrix} \text{Range} \\ \text{Range Difference} \\ \text{Range Difference} \\ \text{Range-Rate} \\ \text{Range-Rate Difference} \\ \text{Range-Rate Difference} \end{bmatrix} = \underline{h}(\underline{x}, \underline{\eta}, \underline{b}, t),$$

and (3), Baker-Nunn cameras, with observation vector

$$\underline{z}(t) = \begin{bmatrix} \text{Right Ascension} \\ \text{Declination} \end{bmatrix} = \underline{h}(\underline{x}, \underline{\eta}, \underline{b}, t).$$

The detailed functional relationship between the observations and the states are presented in Appendix III, where the partial derivatives with respect to states, noise, and biases are developed. Note that all the sensors are affected by time biases, and the Baker-Nunn cameras are affected by a-c time fluctuations as well.

SECTION V

REFERENCES

1. R. A. Nidey, "Gravitational Torque on a Satellite of Arbitrary Shape", ARS Journal, pp. 203-204, February 1960.

2. R. H. Frick and T. B. Garber, "General Equations of Motion of a Satellite in a Gravitational Gradient Field", Rand Report RM-2527, December 1959.

3. T. R. Kane, "Attitude Stability of Earth-Pointing Satellites", AIAA Journal, Volume 3, No. 4, pp. 726-731, April 1965.

4. S. W. McCuskey, Introduction to Advanced Dynamics, Addison - Wesley, Reading, Massachusetts, 1959.

5. "Models for the Analysis of Ground Based Sensors in Determining the Mass of Orbiting Bodies", Report ESD-TR-68-157, Vol I. Electronics Systems Division, U.S. Air Force Systems Command, L.G. Hanscom Field, Bedford, Massachusetts, June 1967. Prepared as Technical Report 1 to Contract F19628-67-C0041 by Westinghouse Surface Division, Baltimore, Maryland.

APPENDIX I

THE COUPLING OF SATELLITE TUMBLING TO ITS ORBITAL MOTION IN A CONSERVATIVE FIELD

Various writers[1,2,3] have considered the problem of the motion of a non-symmetrical satellite in the gravitational field of a major planet. Although the satellite may nominally be travelling in a stable orbit, there is obviously an interaction between the equations which govern the rotational motion of the satellite about its center of mass and the equations of orbital motion. In some cases, interest in this problem centers about the advantageous use of this interaction for purposes of gravity gradient stabilization; in other instances, there is concern about the possibly detrimental effects of this coupling such as excessive tumbling of the satellite, or even significant distortion of the orbital path.

It is one of the purposes of this appendix to show that, in almost any practical situation, these detrimental effects are entirely insignificant. Furthermore, the perturbation of the orbit due to the lack of spherical symmetry of the satellite can almost always be ignored, and the rotational (tumbling) equations can be solved with insignificant error under the assumption that the center of mass of the satellite is moving in a pre-computed orbit. Using this assumption, the tumbling equations for the satellite will be derived in a form which is useful for computational purposes.

In the following derivation, it will be assumed that the satellite is a body of revolution, or at least that two of the three principal moments of inertia are equal. The results, however, leave little doubt that the above claims are equally valid for a body having all three principal moments of

inertia unequal.

In Reference 1, it is shown that the gravitational torque $\underline{N}$ exerted on a body in an "inverse square law" gravity potential field is given by

$$\underline{N} = -(3\mu/r^3)\, \hat{i}_r \times J\hat{i}_r, \tag{I.1}$$

where (x) denotes the vector cross product, and

μ = gravitational constant;

r = distance between centers;

$\hat{i}_r$ = unit radial vector expressed in an $\hat{i}_1$, $\hat{i}_2$, $\hat{i}_3$ coordinate system which is fixed in the body;

J = inertia matrix of the body with respect to the $\hat{i}_1$, $\hat{i}_2$, $\hat{i}_3$ coordinates.

If the $\hat{i}_1$, $\hat{i}_2$, $\hat{i}_3$ coordinates are directed along the principal inertial axes of the body, then J is a diagonal matrix having diagonal elements equal to the principal moments of inertia.

Let $\underline{\omega}$ denote the angular velocity vector with components equal to the angular velocities about the principal axes. Euler's equations of motion describing the rotation of the body have, in this coordinate system, the well-known form [4]

$$J\dot{\underline{\omega}} + \underline{\omega} \times J\underline{\omega} = \underline{N}, \tag{I.2}$$

where the dot denotes differentiation with respect to time. In the case of a body of revolution, we take

$$J = \begin{bmatrix} I & 0 & 0 \\ 0 & I & 0 \\ 0 & 0 & I-\Delta I \end{bmatrix}, \tag{I.3}$$

where ΔI is positive for long cigar-shaped bodies, negative for saucer-shaped bodies.

Let the orthogonal matrix S represent a rotation through an angle β about the symmetric principal axis of the body, and set $\underline{\omega} = S\underline{\lambda}$, or

$$\underline{\omega} = \begin{bmatrix} \cos\beta & \sin\beta & 0 \\ -\sin\beta & \cos\beta & 0 \\ 0 & 0 & 1 \end{bmatrix} \underline{\lambda}.$$

If the angle β is allowed to vary with time, then $\dot{\underline{\omega}} = S\dot{\underline{\lambda}} + \dot{S}\underline{\lambda}$, where

$$\dot{S} = -\dot{\beta} \begin{bmatrix} \sin\beta & -\cos\beta & 0 \\ \cos\beta & \sin\beta & 0 \\ 0 & 0 & 0 \end{bmatrix}.$$

We also introduce the skew symmetric matrix $\boldsymbol{\Omega}$, defined as

$$\boldsymbol{\Omega} = \begin{bmatrix} 0 & -\omega_3 & \omega_2 \\ \omega_3 & 0 & -\omega_1 \\ -\omega_2 & \omega_1 & 0 \end{bmatrix},$$

so that we can write $\underline{\omega} \times J\underline{\omega} = \boldsymbol{\Omega} J\underline{\omega}$. With this notation, (I.2) becomes

$$J(S\dot{\underline{\lambda}} + \dot{S}\underline{\lambda}) + \boldsymbol{\Omega} JS\underline{\lambda} = \underline{N}.$$

Since J obviously commutes with S, S^T and $\dot{S}$, this latter equation can be put into the form

$$J\dot{\underline{\lambda}} + LJ\underline{\lambda} = S^T\underline{N}, \qquad (I.4)$$

with $L = S^T\dot{S} + S^T\boldsymbol{\Omega}S$. If λ_1, λ_2, λ_3 are the components of the vector λ,

we find

$$L = \begin{bmatrix} 0 & \dot{\beta}-\lambda_3 & \lambda_2 \\ -(\dot{\beta}-\lambda_3) & 0 & -\lambda_1 \\ -\lambda_2 & \lambda_1 & 0 \end{bmatrix},$$

and

$$LJ\underline{\lambda} = (I\dot{\beta} - \Delta I\lambda_3) \begin{bmatrix} \lambda_2 \\ -\lambda_1 \\ 0 \end{bmatrix}. \qquad (I.5)$$

With respect to equation (I.1), note that $S^T(\hat{i}_r \times J\hat{i}_r)$ is simply the vector $\hat{i}_r \times J\hat{i}_r$ expressed in the rotated coordinate system having unit vectors $\hat{j}_n = S^T\hat{i}_n$ $(n = 1, 2, 3)$. In this system, the inertia matrix J still has the form (I.3); hence,

$$J\hat{i}_r = I\hat{i}_r - \Delta I(\hat{i}_r \cdot \hat{j}_3)\hat{j}_3$$

in $(\hat{j}_1, \hat{j}_2, \hat{j}_3)$ coordinates, and

$$S^T\underline{N} = 3\mu\Delta I r^{-3}(\hat{i}_r \cdot \hat{j}_3)(\hat{i}_r \times \hat{j}_3)$$

$$= 3\mu\Delta I r^{-3} \begin{bmatrix} (\hat{i}_r \cdot \hat{j}_2)(\hat{i}_r \cdot \hat{j}_3) \\ -(\hat{i}_r \cdot \hat{j}_1)(\hat{i}_r \cdot \hat{j}_3) \\ 0 \end{bmatrix}. \qquad (I.6)$$

Equations (I.4), (I.5) and (I.6) show that $\dot{\lambda}_3 = 0$, or $\lambda_3(t) = \lambda_3(0)$. If we now let $r_n = (\hat{i}_r \cdot \hat{j}_n)$, $n = 1, 2, 3$, we can write the equations of rotational motion in the following simple form.

$$\frac{d}{dt}\begin{bmatrix}\lambda_1\\ \lambda_2\end{bmatrix} = \left(\frac{\Delta I}{I}\lambda_3 - \dot{\beta}\right)\begin{bmatrix}\lambda_2\\ -\lambda_1\end{bmatrix} + \frac{3\mu}{r^3}\frac{\Delta I}{I}\begin{bmatrix}r_2 r_3\\ -r_1 r_3\end{bmatrix}. \tag{I.7}$$

Let us now relate the equation (I.7) to a coordinate system, (n,p,q), having unit vectors with inertially fixed directions, and an origin moving with the satellite. Assume that the satellite is travelling in a simple elliptic orbit. (This will certainly be valid for sufficiently small time intervals; moreover, we intend to show that the perturbation of the orbit due to tumbling is actually negligible over a period of many orbits.) Define the orthogonal unit vectors $\hat{i}_p$, $\hat{i}_q$ and $\hat{i}_n$ as follows:

$\hat{i}_p = \hat{i}_r$ at the instant the satellite is passing through perigee;

$\hat{i}_q$ = unit vector in the direction of instantaneous velocity at perigee;

$\hat{i}_n$ = unit vector normal to the orbital plane, in the direction of the orbit momentum vector.

If v is the true anomaly, then in this fixed-direction system the vector $\hat{i}_r$ has the representation

$$\hat{i}_r = \begin{bmatrix}\cos v\\ \sin v\\ 0\end{bmatrix}. \tag{I.8}$$

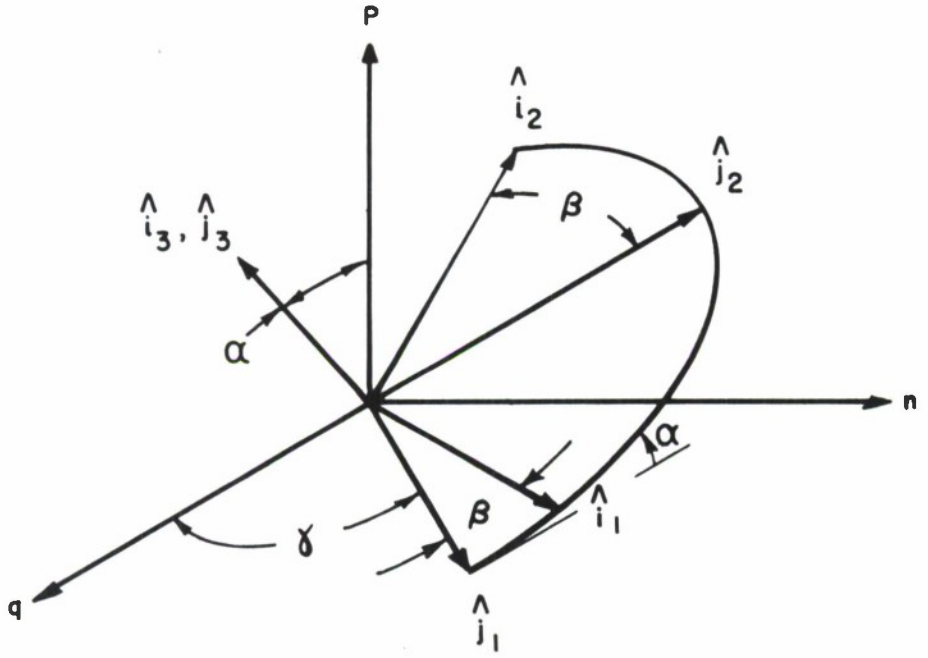

FIGURE 2. TUMBLING GEOMETRY

Figure 2 shows the orientation of the satellite in the fixed system, in terms of both the fixed $\hat{i}_1$, $\hat{i}_2$, $\hat{i}_3$ body coordinates and the rotating $\hat{j}_1$, $\hat{j}_2$, $\hat{j}_3$ coordinates. The angle β has been chosen in such a way that the unit vector $\hat{j}_1$ is in the (q,n) plane. It is clear that

$$\underline{\lambda} = \begin{bmatrix} \dot{\alpha} \\ \dot{\gamma} \sin \alpha \\ \dot{\beta} + \dot{\gamma} \cos \alpha \end{bmatrix} = \text{angular velocities along } (\hat{j}_1, \hat{j}_2, \hat{j}_3). \tag{I.9}$$

In (n,p,q) coordinates, we have

$$\hat{j}_1 = \begin{bmatrix} 0 \\ \cos \gamma \\ \sin \gamma \end{bmatrix}, \qquad \hat{j}_2 = \begin{bmatrix} \sin \alpha \\ -\cos \alpha \sin \gamma \\ \cos \alpha \cos \gamma \end{bmatrix}, \qquad \hat{j}_3 = \begin{bmatrix} \cos \alpha \\ \sin \alpha \sin \gamma \\ -\sin \alpha \cos \gamma \end{bmatrix}, \tag{I.10}$$

and we find

$$r_1 = \cos \gamma \sin v = \hat{i}_r \cdot \hat{j}_1$$

$$r_2 = \sin \alpha \cos v - \cos \alpha \sin \gamma \sin v = \hat{i}_r \cdot \hat{j}_2$$

$$r_3 = \cos \alpha \cos v + \sin \alpha \sin \gamma \sin v = \hat{i}_r \cdot \hat{j}_3 \tag{I.11}$$

If a and e are, respectively, the semi-major axis and the eccentricity of the orbit, it is well known that

$$r = \frac{a(1-e^2)}{1 + e \cos v} . \tag{I.12}$$

Noting finally that $(\Delta I\lambda_3 - I\dot{\beta}) = (\Delta I - I)\lambda_3 + I\dot{\gamma}\cos\alpha$, it follows from equations (I.9), (I.11) and (I.12) that the tumbling equations (I.7) can be written in terms of the physically meaningful angles α, γ and v, and the constant λ_3. It is of particular importance that, in their final form, these equations are entirely independent of the angle β, which in the case of a body of revolution is an unobservable quantity.

The kinetic energy of rotation is given by

$$T = (1/2)\underline{\lambda}^T J\underline{\lambda} = (1/2)\underline{\omega}^T(SJS^T)\underline{\omega} = (1/2)\underline{\omega}^T(JSS^T)\underline{\omega} = (1/2)\underline{\omega}^T J\underline{\omega}. \qquad (I.13)$$

Differentiation with respect to T produces

$$\dot{T} = \underline{\lambda}^T J\dot{\underline{\lambda}}, \qquad (I.14)$$

which may be regarded as either the rate of increase of the rotational energy of the satellite, or the rate of decrease of energy in the orbit. Premultiplying (I.4) by $\underline{\lambda}^T$, and noting that $\underline{\lambda}^T LJ\underline{\lambda} = 0$, we find

$$\begin{aligned}\dot{T} &= \underline{\lambda}^T S^T \underline{N} \\ &= \frac{3\mu}{r^3}\,\Delta I\, r_3\,(\lambda_1 r_2 - \lambda_2 r_1), \qquad (I.15)\end{aligned}$$

where the latter expression follows from (I.6).

In order to justify the previous statements concerning the tumbling rates and the perturbation of the orbit due to tumbling, it would be sufficient to show that the change in T over a period of several orbits is negligible both with respect to the total orbital energy and the implied change in tumbling rate. The direct computation of the energy or the energy rate, however, would

essentially require the solution of the nonlinear tumbling equations (I.7), and this problem is extremely difficult if not intractable.

Consider, instead, the following hypothetical situation. Suppose that the satellite is equipped with a set of torque rockets which can produce arbitrary rotations, but no translational motion, of the satellite. Suppose, in addition, that these rockets are either pre-programmed or controlled by an intelligent being in such a way that the total decrease in orbital energy over a pre-specified time interval is maximized. It is assumed that the rockets are capable of producing both continuous and impulsive outputs, so that there are no inertial limitations on the possible rotational motions of the satellite.

Since the equations (I.7) no longer govern the satellite rotations, (I.15) does not represent the rate of increase of rotational energy, but (I.15) is still the correct expression for the rate of decrease of orbital energy. Furthermore, the maximum decrease in orbital energy under the artificial motion described above is an upper bound for both the actual decrease in orbital energy and the actual increase in rotational energy under any natural motion of the satellite.

Since we are still assuming motion in a nominal elliptic orbit, we can treat T, α and γ as functions of time t or, equivalently, as functions of the true anomaly v. Noting equations (I.9) and (I.12), we rewrite (I.15) as

$$\frac{dT}{dv} = \frac{3\mu(1+e\cos v)^3}{a^3(1-e^2)^3}\,\Delta I\, r_3\left[r_2\frac{d\alpha}{dv} - r_1 \sin\alpha \frac{d\gamma}{dv}\right], \tag{I.16}$$

where r_1, r_2 and r_3 are still given by (I.11). Our plan is now to integrate (A.16) between specified values of v, and to maximize the resulting expression

with respect to the unknown functions $\alpha(v)$ and $\gamma(v)$. For simplicity, we will work with the absolute value $|\Delta I|$. Without displaying all of the cumbersome details, we state that the function $\gamma(v)$ which produces a maximum for this integral is simply $\gamma(v) = \pi/2$. This can be obtained either as a solution of the Euler-Lagrange equation[4] which is associated with this variational problem, or by recognizing that $\underline{\lambda}^T(\hat{i}_r \times J\hat{i}_r)$ is largest when the angular velocity about an axis in the direction of $\hat{i}_r \times \hat{j}_3$ is a maximum, and this occurs when $\gamma = \pi/2$.

Setting $\gamma(v) = \pi/2$ in (I.16), and substituting for r_2 and r_3, we obtain

$$\frac{dT}{dv} = \frac{3\mu(1+e\cos v)^3}{2a^3(1-e^2)^3} |\Delta I| \sin 2(\alpha - v) \frac{d\alpha}{dv}, \tag{I.17}$$

Integrating this expression between limits v_1 and v_2, we are left with a simple calculus of variations problem in the single unknown function $\alpha(v)$. The associated Euler-Lagrange equation is algebraic, and leads to the result

$$\tan 2(\alpha - v) = \frac{-2(1+e\cos v)}{3e \sin v}. \tag{I.18}$$

From (I.18), we compute

$$\frac{d\alpha(v)}{dv} = 1 + \frac{3e(e+\cos v)}{(3e\sin v)^2 + 4(1+e\cos v)^2},$$

and

$$\sin 2(\alpha - v) = \frac{2(1+e\cos v)}{\left[(3e\sin v)^2 + 4(1+e\cos v)^2\right]^{1/2}}.$$

Clearly when $e < 4/7$, we must choose the positive sign for $\sin 2(\alpha - v)$, since the expression for $d\alpha/dv$ is positive for all v in this case. Actually, a closer analysis shows that the positive sign should be chosen for all $e < 1$, but the simpler observation is sufficient for practical purposes.

At the endpoints of the interval of integration, if the angle $\alpha(v)$ does not satisfy equation (I.18), an impulse from our hypothetical rockets can be used to bring the satellite into position. Inspection of (I.17) leads to the conclusion that, if the integration is performed over an integer number of orbits, the maximum contribution to the integral due to endpoint effects is given by

$$T_{ep} \leq \frac{3\mu|\Delta I|}{a^3(1-e)^3} . \tag{I.19}$$

Substituting the expressions for $\sin 2(\alpha - v)$ and $d\alpha/dv$ into (A.17) and integrating over a single orbit, we find

$$\frac{\Delta T}{\text{orbit}} \leq \frac{3\mu\pi|\Delta I|}{a^3(1-e^2)^3} F(e),$$

where

$$F(e) = \frac{1}{\pi} \int_0^{\pi} \frac{2(1+e\cos v)^4\left[(3e\sin v)^2 + 4(1+e\cos v)^2 + 3e(e+\cos v)\right]}{\left[(3e\sin v)^2 + 4(1+e\cos v)^2\right]^{3/2}}\, dv .$$

The following table shows the results of a numerical integration for the function F(e), as well as a tabulation of the values of $1 + 2e^2$.

e	F(e)	$1+2e^2$
0	1.000	1.000
0.1	1.021	1.020
0.3	1.184	1.180
0.5	1.503	1.500
0.7	1.970	1.980
1.0	2.939	3.000

Hence, we have the very simple estimate

$$\frac{\Delta T}{\text{orbit}} \leq \frac{3\mu\pi|\Delta I|}{a^3}\frac{(1+2e^2)}{(1-e^2)^3} \quad . \tag{I.20}$$

Combining the results (I.19) and (I.20), we obtain the following upper bound for the decrease in orbital energy, and the corresponding increase in tumbling energy, over a period of n orbits.

$$|\Delta T(n)| \leq \frac{3\mu|\Delta I|}{a^3}\left[\frac{(1+e)^3 + n\pi(1+2e^2)}{(1-e^2)^3}\right]. \tag{I.21}$$

Since the total energy of the orbit is, initially, $h = m\mu/2a$, where m is the mass of the satellite, the fractional change in orbital energy per orbit (neglecting endpoint effects) is no greater than

$$\frac{\Delta h}{h} \leq \frac{6\pi}{a^2}\,\frac{|\Delta I|}{m}\,\frac{(1+2e^2)}{(1-e^2)^3} \quad . \tag{I.22}$$

For the extreme case of a cylindrical satellite having length L and radius $R \ll L$, this becomes

$$\frac{\Delta h}{h} \leq \frac{\pi}{2} \left(\frac{L}{a}\right)^2 \frac{(1+2e^2)}{(1-e^2)^3} \quad . \tag{I.23}$$

For an earth orbit, we must have $a(1-e) > 2 \times 10^7$ ft. Also, for $0 \leq e \leq 0.8$, the inequality $(1+2e^2)/(1+e)^3(1-e) < 2$ is valid. Hence, over the stated range for e, we have $\Delta h/h < 10^{-14} L^2$, where L is the length, in feet, of the cylindrical satellite.

Assume now that the decrease in orbital energy over a single orbit corresponds to an increase of $I(\Delta\omega)^2/2$ units of energy due to a change in the angular velocity of the cylindrical satellite about some non-symmetric principal axis. In this case, we must have

$$(\Delta\omega)^2 \leq \frac{6\pi\mu}{[a(1-e)]^3} \frac{|\Delta I|}{I} \frac{(1+2e^2)}{(1+e)^3} \quad . \tag{I.24}$$

Noting that $|\Delta I|/I < 1$ for any cylinder and $(1+2e^2)/(1+e)^3 \leq 1$ for $e \geq 0$, we take $\mu = 1.4 \times 10^{16}$ ft.^{3}/sec.^{2} and the above inequality for a(1-e) to obtain

$$(\Delta\omega)^2 < 33 \times 10^{-6} \text{ rad.}^2/\text{sec.}^2 \tag{I.25}$$

for a complete orbit. This estimate is extremely conservative, since the satellite cannot tumble end over end and simultaneously maintain a configuration which causes the orbital energy to decrease at each instant. The main value of the estimate (I.25) is in demonstrating that, over the small portion of an

orbit which lies within the range of a single tracking station, the net change in angular velocity due to gravitational effects is rather small.

APPENDIX II

PERTURBATIONS ON CYLINDRICAL SATELLITES DUE TO SOLAR RADIATION PRESSURE

A. GENERAL

There are three components of solar radiation force acting on a satellite:

(1) That due to energy impinging directly from the sun and reflected from the earth.

(2) That due to the reaction of specularly reflecting radiation from the satellite.

(3) That due to the reaction of diffusely scattering radiation from the satellite.

As noted in Appendix I of Reference 5, if the incident radiation approaches from the direction $\hat{i}_i$ shown in Figure 3 below, then the pressure exerted normal to $\hat{i}_i$ is

$$\underline{p} = (I_s/c)\,\hat{i}_i = p\,\hat{i}_i, \tag{II.1}$$

where I_s is the irradiance and c is the speed of light. When $\underline{p}$ impinges upon a differential surface area $d\underline{A}$, the differential force due to the incident flux is

$$d\underline{F}_{in} = \hat{i}_i\,(\underline{p} \cdot d\underline{A}) = \hat{i}_i\,(I_s/c)\,(\hat{i}_i \cdot d\underline{A}), \tag{II.2}$$

while the differential force due to the flux being reflected back from the surface is

$$d\underline{F}_{refl} = -\hat{i}_{refl}\,(I_r/c)\,(\hat{i}_{refl} \cdot d\underline{A}), \tag{II.3}$$

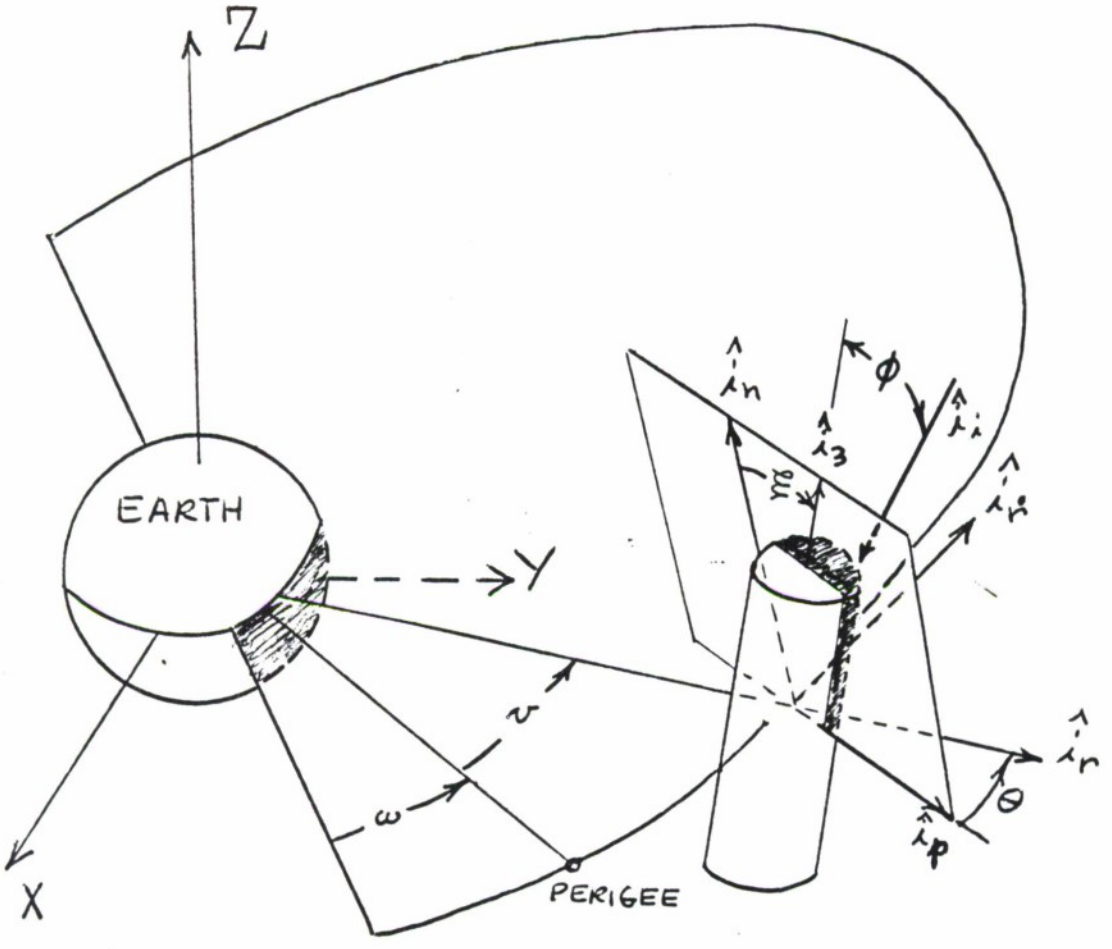

FIGURE 3. TUMBLING CONFIGURATION

where $\hat{i}_{refl}$ is the unit vector in the direction of the reflected flux and I_r is the irradiance in that direction.

The net solar force due to direct solar radiation is the integral of (II.2) plus (II.3).

Now, the total pressure $\underline{p}$ at the satellite consists of a part directed from the sun and a part reflected from the earth. For simplicity, this pressure vector will be resolved into components in the $\hat{i}_r$ and $\hat{i}_{ss}$ directions, i.e., radial from earth and sun-to-satellite, respectively. This pressure vector can be written as

$$\underline{p} = (I_s/c)\ (p_1\ \hat{i}_r + p_2\ \hat{i}_{ss}), \qquad \text{(II.4)}$$

where, to a good approximation, [5]

$$p_1 = \begin{cases} \lambda q\ (a_1 + a_2)\cos\alpha & , \quad |\alpha| \leq \pi/2 - B_\lambda \\ \lambda q\ a_r & , \quad \pi/2 - B_\lambda \leq |\alpha| \leq \pi/2 + B_\lambda \\ 0 & , \quad \pi/2 + B_\lambda \leq |\alpha| \leq \pi \end{cases}$$

$$p_2 = \begin{cases} (1 + \lambda q a_2) & , \quad |\alpha| \leq \pi/2 - B_\lambda \\ (1 + \lambda q a_{ss}) & , \quad \pi/2 - B_\lambda \leq |\alpha| \leq \pi/2 + B_\lambda \\ 0 & , \quad \pi/2 + B_\lambda \leq |\alpha| \leq \pi \end{cases}$$

given that

q = Earth albedo,

λ = ratio of earth radius to distance between satellite and center of earth

$B_\lambda = \arccos \lambda$,

$$a_1 = (-.0417 + .5431\lambda)/3,$$

$$a_2 = \left\{.0444 - 3.17(\lambda - .77)^3 + .0045\,(\lambda - .77)\,\sin\left[14.3(\lambda - .77)\pi\right]\right\}/3$$

$$a_{ss} = a_2\left[1 + s - se^{s\tau y} - e^{-\tau}y\,(2 + sy)\right]/2$$

$$a_r = \left\{a_{ss} + (a_1/2)\left[s + 1 - s(1 + sy)^d\right]\right\}\cos\alpha$$

$$+\left\{\frac{\lambda^2\left[(1/\lambda - \sin\alpha)^3 + (\lambda - \sin\alpha)^3\right]}{(1+\lambda^2 - 2\lambda\sin\alpha)^{3/2}} - \frac{(1-\lambda^2)^{3/2}}{\lambda}\right\}\frac{\sin\alpha}{6},$$

$$\tau = -4 + 9.3\lambda$$

$$y = (\alpha - \pi/2)/\beta_\lambda$$

$$s = \begin{cases} 1, & y \le 0, \\ -1, & y > 0, \end{cases}$$

$$d = 3.7 + 59(\lambda - .77)^2 .$$

B. NET RADIATION FORCES

1. Incident Radiation

Neglecting the reflection effects, the impinging energy will produce a net force in the $\hat{i}_i$ direction defined by the integration of (II.2) over the surface A_s of the satellite:

$$\underline{F}_{in} = \int_{A_s} d\underline{F}_{in} = \underline{P}\left[\int_{A_b} \hat{i}_i \cdot d\underline{A}_b + \int_{A_l} \hat{i}_i \cdot d\underline{A}_l\right], \qquad (II.6)$$

where

$A_b = \pi R_c^2$, the area of the base of a cylinder of radius R_c,

$A_l = 2LR_c$, cross-sectional area normal to the base of a cylinder length L.

Taking the unit vector $\hat{i}_3$ to be normal to the base of the cylinder, (see Figure 3), and defining

$$\cos\phi = -(\hat{i}_i \cdot \hat{i}_3),$$

where $\hat{i}_3 = \sin\xi\ \hat{i}_p + \cos\xi\ \hat{i}_n$,

we find that (II.6) becomes

$$\underline{F}_{in} = \underline{p}\ (A_b\ |\ \cos\phi\ |\ + A_1\ |\ \sin\phi\ |\ ). \qquad \text{(II.7)}$$

2. Specularly Reflected Radiation

Consider a ray of light which is reflected from an increment $d\underline{A}$ of surface area according to Snell's Law. If the ray impinges at an angle $0 \leq \psi_n \leq \pi/2$ with the normal, then it will leave at an angle ψ_n with the normal, as shown in Figure 4 below. If the specular

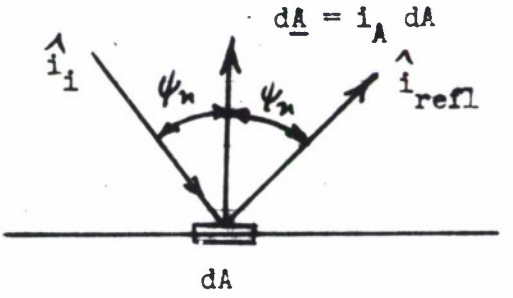

FIGURE 4. SPECULAR REFLECTION

reflection coefficient is defined to be k_r, then the reflection irradiance is $I_r = k_r\ I_s$, and the integration of (II.3) yields

$$\underline{F}_{refl} = -k_r p \left[\int_{A_b} \hat{i}_{refl}\ (\hat{i}_{refl} \cdot d\underline{A}) + \int_{A_{side}} \hat{i}_{refl}\ (\hat{i}_{refl} \cdot d\underline{A}) \right] \qquad \text{(II.8)}$$

Now, over the base of the cylinder,

$$d\underline{A} = \hat{i}_3\ \text{sign}\ (\cos\phi)\ dA\ , \qquad \text{(II.9)}$$

where

$$\text{sign}\ (x) = \begin{cases} -1\ , & x \leq 0 \\ +1\ , & x > 0 \end{cases}$$

the sign function being necessary to distinguish whether the top base

of the bottom base of the cylinder is exposed to the light. If $\hat{i}_A$ is the normal to dA, it is clear from Figure 4 that

$$\hat{i}_{refl} = \hat{i}_i + 2(\cos \psi_n)\, \hat{i}_A. \tag{II.10}$$

But from Figure 3 we see that

$$\cos \psi_n = |\cos \phi|,$$

so that (II.10) becomes

$$\begin{aligned} \hat{i}_{refl} &= \hat{i}_i + 2\,|\cos\phi|\ \mathrm{sign}(\cos\phi)\ \hat{i}_3 \\ &= \hat{i}_i + 2\cos\phi\ \hat{i}_3. \end{aligned} \tag{II.11}$$

Hence, over the base area,

$$\begin{aligned} \hat{i}_{refl} \cdot d\underline{A} &= (-|\cos\phi| + 2|\cos\phi|)\ dA \\ &= |\cos\phi|\ dA. \end{aligned} \tag{II.12}$$

Combining (II.11) and (II.12) in the first integral in (II.8), we have

$$\int_{A_b} \hat{i}_{refl}\ (\hat{i}_{refl} \cdot d\underline{A}) = A_b\ |\cos\phi|(\hat{i}_i + 2\cos\phi\ \hat{i}_3). \tag{II.13}$$

Now, integrating over the side surface of the cylinder, we note that we can decompose $\underline{p}$ into two parts: One part tangential to the longitudinal

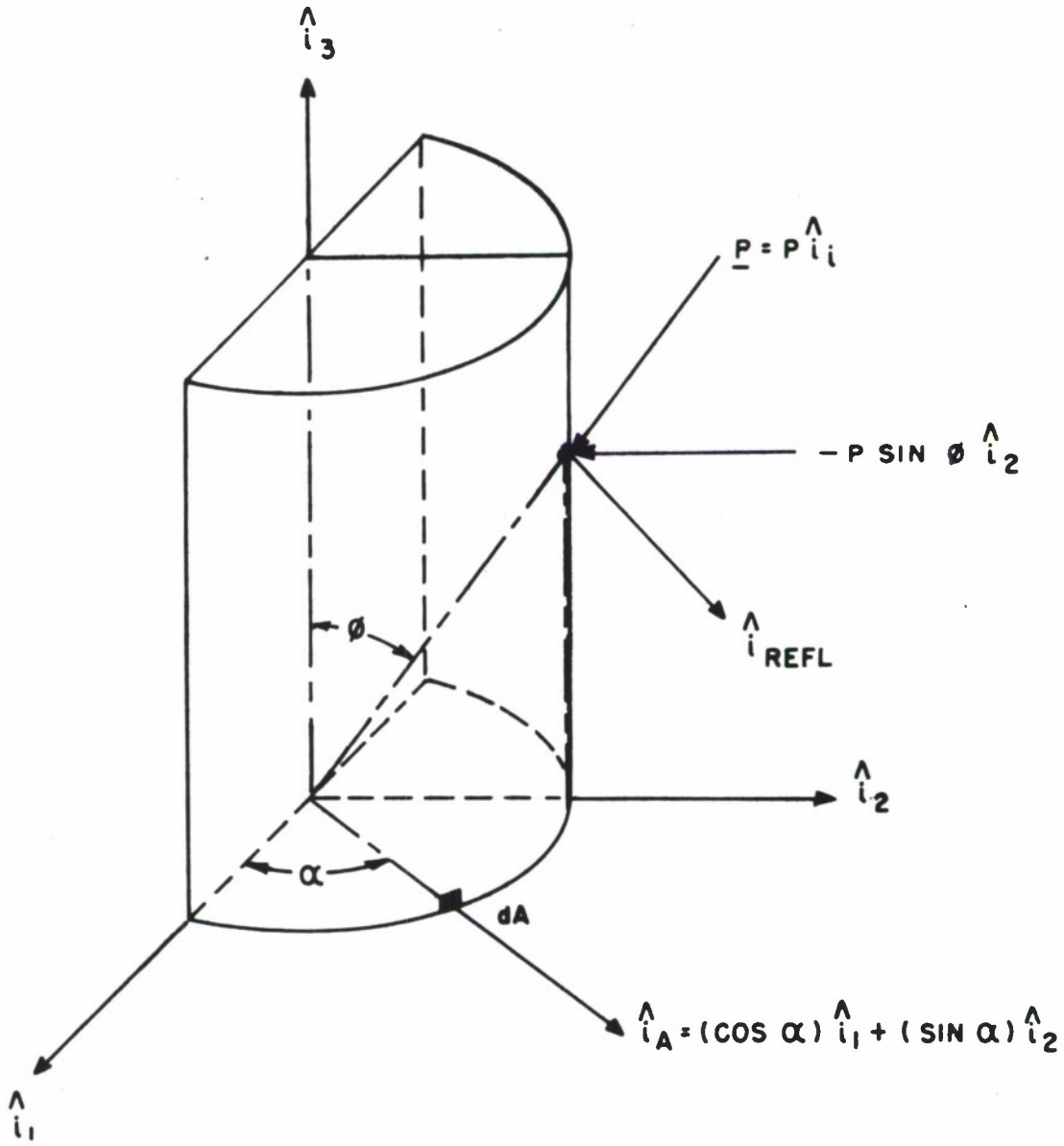

FIGURE 5. SPECULAR REFLECTION FROM CYLINDER WALL

axis and one part normal to that axis. Figure 5 provides the details. Only the normal part of p, that having direction cosine - sin ϕ/ $\hat{i}_2$, appears in the dot product

$$\hat{i}_{refl} \cdot \hat{i}_A = -\hat{i}_i \cdot \hat{i}_A,$$

so that

$$\hat{i}_{refl} \cdot \hat{i}_A = \sin \phi \sin \alpha, \; 0 \leq \phi \leq \pi, \tag{II.14}$$

where α is the polar reference angle to $\hat{i}_A$. The full unit vector $\hat{i}_{refl}$ also is needed. Referral to Figure 6, below, where the origin has been moved to the surface increment dA of the previous figure, provides

$$\hat{i}_{refl} = (\sin \phi)(\sin 2\alpha)\, \hat{i}_1 - (\sin \phi)(\cos 2\alpha)\, \hat{i}_2 - (\cos \phi)\, \hat{i}_3. \tag{II.15}$$

Substituting (II.14) and (II.15) into the second integral in (II.8), we find

$$\begin{aligned} \int_{A_{side}} \hat{i}_{refl}\, (\hat{i}_{refl} \cdot d\underline{A}) &= \int_0^{\pi} \left[(\sin \phi)(\sin 2\alpha)\, \hat{i}_1 \right. \\ &\left. - (\sin \phi)(\cos 2\alpha)\, \hat{i}_2 - (\cos \phi)\, \hat{i}_3 \right] (\sin \phi)(\sin \alpha)\, R_c L d\alpha, \\ &= - A_1 \left(- \frac{\sin^2 \phi}{3}\, \hat{i}_2 + (\cos \phi)(\sin \phi)\, \hat{i}_3\right), \\ &= - \frac{A_1 \sin \phi}{3} \left[4(\cos \phi)\, \hat{i}_3 + \hat{i}_i\right], \\ &0 \leq \phi \leq \pi. \end{aligned} \tag{II.16}$$

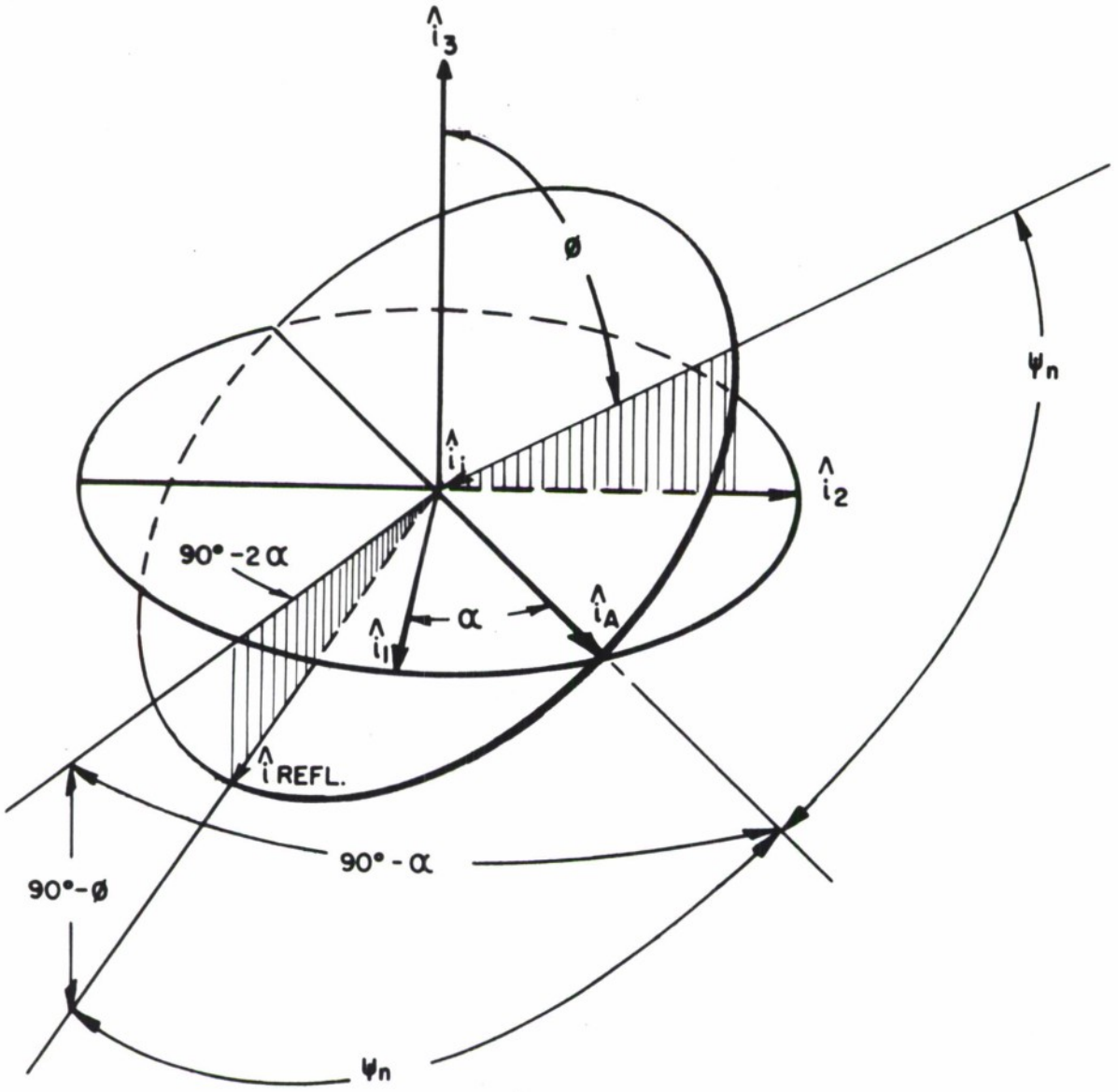

FIGURE 6. GEOMETRY FOR DIRECTION COSINES OF $\hat{i}_{refl}$, SPECULAR CASE.

The net specular reflection force now follows from putting (II.13) and (II.16) into (II.8):

$$\underline{F}_{refl} = - k_r\, p \left[\left\{ A_b |\cos \phi| - (A_1/3)|\sin \phi| \right\} \hat{i}_i \right.$$

$$\left. + 2 \cos \phi \left\{ A_b |\cos \phi| - (2A_1/3)|\sin \phi| \right\} \hat{i}_3 \right] . \qquad \text{(II.17)}$$

3. Diffusely Reflected Radiation

For the case of diffuse radiation, the reflected energy obeys Lambert's Law. As developed in Appendix I of Reference 5, the differential reaction force is normal to any increment of area dA:

$$d\underline{F}_{refl} = \hat{i}_A \; (2/3)\, (k_d I_{s/c})\, (\hat{i}_i \cdot d\underline{A}), \qquad \text{(II.18)}$$

where k_d is the diffuse reflection coefficient. Again

$$\underline{F}_{refl} = \int_{A_b} d\underline{F}_{refl} + \int_{A_{side}} d\underline{F}_{refl} \; . \qquad \text{(II.19)}$$

For the base,

$$\int_{A_b} d\underline{F}_{refl} = - (2/3)(k_d I_s/c)\, A_b \cos \phi \, \hat{i}_3 .$$

For the side, (II.14) can be used to obtain

$$\int_{A_{side}} d\underline{F}_{refl} = -(2/3)(k_d I_s/c)(\sin \phi) \int_0^{\pi} \left[(\cos \alpha)\hat{i}_1 + (\sin \alpha)\hat{i}_2\right] (\sin \alpha)\, R_c L\, d\alpha,$$

$$= -A_1(\pi/6)(k_d I_s/c)(\sin \phi)\hat{i}_2,$$

$$= A_1(\pi/6)(k_d I_s/c)(\hat{i}_i + \cos \phi\, \hat{i}_3).$$

Hence, for diffuse reflection,

$$\underline{F}_{refl} = (k_d\, p/3) \left[(\pi A_1/2)\hat{i}_i + \{(\pi A_1/2) - 2A_b\}(\cos \phi)\hat{i}_3\right] . \quad \text{(II.20)}$$

C. FINAL RESULTS

Combining (II.7), (II.17), and (II.20), and upon dividing by the mass m, we obtain finally, after using (II.4) to substitute for $\underline{p}$ (or $\hat{i}_i$),

$$\ddot{\underline{r}}_{solar} = (I_s/c)\,(A_1/m) \Big[\left[(A_b/A_1)\,(1-k_r)\,|\cos \phi\,| + \pi k_d/6 + (1 + k_r/3)\,|\sin \phi\,|\right]\left[p_1 \hat{i}_r + p_2 \hat{i}_{ss}\right]$$
$$+ \left[2\,(A_b/A_1)\,(k_r\,|\cos \phi\,| + k_d/3) - (4/3)k_r\,|\sin \phi\,| - \pi k_d/6\right]\left[\, p_1 \cos \alpha_r + p_2 \cos \alpha_s \,\right] \hat{i}_3 \Big], \quad \text{(II.21)}$$

where

$$\cos \alpha_s = \hat{i}_{ss} \cdot \hat{i}_3 \ ,$$

$$\cos \alpha_r = \hat{i}_r \cdot \hat{i}_3 \ ,$$

$$\cos \phi = (p_1 \cos \alpha_r + p_2 \cos \alpha_s) / \sqrt{p_1^2 + p_2^2}$$

The last identity follows from the fact that

$$\cos \phi = \hat{i}_i \cdot \hat{i}_3$$

and from (II.4), which yields

$$\hat{i}_i = (p_1 \hat{i}_r + p_2 \hat{i}_{ss}) / \sqrt{p_1^2 + p_2^2}$$

APPENDIX III

OBSERVATION EQUATIONS

The notation used in this appendix in some cases contradicts the definitions for the same symbols used elsewhere in this report and in Reference 5. This occurs because particular symbols are commonly accepted to mean one thing in orbital mechanics, and something entirely different in radar technology.

The symbol definitions within this appendix which are to be interpreted locally only are the following:

R = range

$\dot{R}$ = range-rate,

A = Azimuth,

E = elevation,

α = right ascension

δ = declination,

$\underline{r}_s$ = station location in inertial geocentric coordinates,

ΔR_i = range differences, $i = 1,2$,

$\Delta \dot{R}_i$ = range-rate differences,

φ ,θ' = defined forms of station latitude and longitude.

A. MONOSTATIC RADARS

The monostatic radars to be evaluated in this study measure range R, range-rate $\dot{R}$, azimuth A, and elevation E. Given the state vector $\underline{x}(t)$ and the station location vector

$$\underline{r}_s = \begin{bmatrix} x_s \\ y_s \\ z_s \end{bmatrix}$$

in inertial coordinates, and given the inertial spin rate of the earth ω_e, we can write explicitly the entries of the monostatic observation vector

$$\underline{z}(t) = \begin{bmatrix} R \\ \dot{R} \\ A \\ E \end{bmatrix} = \underline{h}\,(\underline{x},\ \underline{\eta},\ \underline{b},\ t). \qquad \text{(III.1)}$$

These are

$$R = \sqrt{(x - x_s)^2 + (y - y_s)^2 + (z - z_s)^2}\ ,$$

$$\dot{R} = (1/R)\left[\,(x - x_s)(\dot{x} + \omega_e y_s) + (y - y_s)(\dot{y} - \omega_e x_s) + (z - z_s)\dot{z}\,\right],$$

$$A = \tan^{-1}\left[\frac{y'''}{-x'''}\right]\ ,$$

$$E = \tan^{-1}\left[\frac{z'''}{\sqrt{R^2 - (z''')^2}}\right]\ , \qquad \text{(III.2)}$$

where

$$\begin{bmatrix} x''' \\ y''' \\ z''' \end{bmatrix} = \begin{bmatrix} \sin\varphi \cos\Theta' & \sin\varphi \sin\Theta' & -\cos\varphi \\ -\sin\Theta' & \cos\Theta' & 0 \\ \cos\varphi \cos\Theta' & \cos\varphi \sin\Theta' & \sin\varphi \end{bmatrix} \begin{bmatrix} x - x_s \\ y - y_s \\ z - z_s \end{bmatrix}$$

$$\sin\varphi = z_s / \sqrt{x_s^2 + y_s^2 + z_s^2} \quad , \qquad \text{(latitude)}$$

$$\sin\Theta' = y_s / \sqrt{x_s^2 + y_s^2} \quad . \qquad \text{(longitude)}$$

Then

$$\partial R/\partial \underline{x} = (1/R) \left[x - x_s,\ y - y_s,\ z - z_s,\ 0,\ 0,\ 0 \right] ,$$

$$\partial \dot{R}/\partial \underline{x} = (1/R) \left[\frac{R(\dot{x}+\omega_e y_s) - \dot{R}(x-x_s)}{R},\ \frac{R(\dot{y}-\omega_e x_s) - \dot{R}(y-y_s)}{R} , \right.$$

$$\left. \frac{R\dot{z} - \dot{R}(z-z_s)}{R},\ x-x_s,\ y-y_s,\ z-z_s \right] ,$$

$$\partial A/\partial \underline{x} = \frac{1}{R^2-(z''')^2} \left[(-x''' \sin\Theta' - y''' \cos\Theta' \sin\varphi),\ (x''' \cos\Theta' \right.$$

$$\left. - y''' \sin\Theta' \sin\varphi),\ y''' \cos\varphi,\ 0,\ 0,\ 0 \right] ,$$

$$\partial E/\partial \underline{x} = \frac{1}{\sqrt{R^2 - (z''')^2}} \left[\left\{ \cos\Theta' \cos\varphi - (z'''/R^2)(x-x_s) \right\} , \right.$$

$$\left\{ \sin\Theta' \cos\varphi - (z'''/R^2)(y-y_s) \right\} ,$$

$$\left. \left\{ \sin\varphi - (z'''/R^2)(z-z_s) \right\} ,\ 0,\ 0,\ 0 \right] ,$$

(III.3)

which are to be used in

$$H = \begin{bmatrix} \partial R/\partial \underline{x} \\ \partial \dot{R}/\partial \underline{x} \\ \partial A/\partial \underline{x} \\ \partial E/\partial \underline{x} \end{bmatrix} \qquad \text{(III.4)}$$

The noise matrix H_η is the 4 X 4 identity matrix

$$H_\eta = \begin{bmatrix} 1 & & & \\ & 1 & & \\ & & 1 & \\ & & & 1 \end{bmatrix} , \qquad \text{(III.5)}$$

and the bias matrix H_b is the 4 X 8 array

$$H_b = \left[\begin{array}{cccc:c:c} 1 & & & & & \\ & 1 & & & \dfrac{\partial \underline{h}}{\partial \underline{r}_s}\, T(t) & \dfrac{\partial \underline{h}}{\partial t} \\ & & 1 & & & \\ & & & 1 & & \end{array}\right] , \qquad \text{(III.6)}$$

which associates with the bias 8-vector

$$\underline{b} = \begin{bmatrix} \text{Range Bias} \\ \text{Range-Rate Bias} \\ \text{Azimuth Bias} \\ \text{Elevation Bias} \\ x^1 \text{ Station Location Bias} \\ y^1 \text{ Station Location Bias} \\ z^1 \text{ Station Location Bias} \\ \text{Clock Bias} \end{bmatrix} \qquad \text{(III.7)}$$

Now, the station location biases are given in an earth-fixed coordinate system and are constant in that system. Defining the earth-fixed system $\underline{r}^1$ = column (x^1, y^1, z^1) used in Appendix III of Reference 5, we have that

$$\underline{r} = T(t)\, \underline{r}^1 = PNG\, \underline{r}^1,$$

where P, N, and G are orthogonal matrices that account respectively for the earth's precession, nutation, and rotation about its polar axis.

Note that $\frac{\partial \underline{h}}{\partial \underline{r}_s}$ is composed of the rows

$$\begin{aligned}
\partial R/\partial \underline{r}_s &= -\partial R/\partial \underline{r}, \\
\partial \dot{R}/\partial \underline{r}_s &= -\frac{1}{R^2}\Big[\big[R(\dot{x} + \omega_e y) - \dot{R}(x-x_s)\big] , \\
&\qquad \big[R(\dot{y}-\omega_e x) - \dot{R}(y-y_s)\big], \big[R\dot{z} - \dot{R}(z-z_s)\big]\Big] \\
\partial A/\partial \underline{r}_s &= -\partial A/\partial \underline{r}, \\
\partial E/\partial \underline{r}_s &= -\partial E/\partial \underline{r}, \qquad \text{(III.8)}
\end{aligned}$$

where $\frac{\partial}{\partial \underline{r}}$ is the 3-element row vector in $\frac{\partial}{\partial \underline{x}} = \left[\frac{\partial}{\partial \underline{r}} \;\vdots\; \frac{\partial}{\partial \dot{\underline{r}}}\right]$.

The timing-bias part of (III.6), $\partial \underline{h}/\partial t$, is a column array of the following scalar partials:

$$\begin{aligned}
\partial R/\partial t &= (\partial R/\partial \underline{r})\, \dot{\underline{r}} + (\partial R/\partial \underline{r}_s)\, \dot{\underline{r}}_s , \\
\partial \dot{R}/\partial t &= (\partial \dot{R}/\partial \underline{x})\, \dot{\underline{x}} + (\partial \dot{R}/\partial \underline{r}_s)\, \dot{\underline{r}}_s , \\
\partial A/\partial t &= (\partial A/\partial \underline{r})\, \dot{\underline{r}} + (\partial A/\partial \underline{r}_s)\, \dot{\underline{r}}_s , \\
\partial E/\partial t &= (\partial E/\partial \underline{r})\, \dot{\underline{r}} + (\partial E/\partial \underline{r}_s)\, \dot{\underline{r}}_s , \qquad \text{(III.9)}
\end{aligned}$$

where $\dot{\underline{r}} = \begin{bmatrix} x_4 \\ x_5 \\ x_6 \end{bmatrix}$,

$$\dot{\underline{r}}_s = \begin{bmatrix} -y_s \\ x_s \\ 0 \end{bmatrix} \omega_e .$$

B. TRI-STATIC RADARS

The tri-static radars provide a range and range-rate measurement R and $\dot{R}$ from one site, and the differences $\Delta R_1 = R-R_1$, $\Delta R_2 = R-R_2$, $\Delta\dot{R}_1 = \dot{R} - \dot{R}_1$, $\Delta\dot{R}_2 = \dot{R} - \dot{R}_2$ calculated with respect to the ranges and range-rates R_1, R_2 and $\dot{R}_1$, $\dot{R}_2$ to two other sites. The observation vector is now

$$\underline{z}(t) = \begin{bmatrix} R \\ \Delta R_1 \\ \Delta R_2 \\ \dot{R} \\ \Delta\dot{R}_1 \\ \Delta\dot{R}_2 \end{bmatrix} = \underline{h}\,(\underline{x},\ \underline{\eta},\ \underline{b},\ t). \qquad \text{(III.10)}$$

If the three sites are located respectively at

$$\underline{r}_s = \begin{bmatrix} x_s \\ y_s \\ z_s \end{bmatrix}, \qquad \underline{r}_{s1} = \begin{bmatrix} x_{s1} \\ y_{s1} \\ z_{s1} \end{bmatrix}, \qquad \underline{r}_{s2} = \begin{bmatrix} x_{s2} \\ y_{s2} \\ z_{s2} \end{bmatrix}$$

then R and $\dot{R}$ are the same as in the monostatic case, whereas

$$\Delta R_i = R - \sqrt{(x-x_{si})^2 + (y-y_{si})^2 + (z-z_{si})^2},$$

$$\Delta\dot{R}_i = \dot{R} - \frac{1}{R-\Delta R_i}\Big[(x-x_{si})\,(\dot{x} + \omega_e y_{si})$$

$$+ (y-y_{si})\,(\dot{y}-\omega_e x_{si}) + (z-z_{si})\,\dot{z}\Big],$$

$$i = 1,2. \qquad \text{(III.11)}$$

The state partials $\partial R/\partial \underline{x}$ and $\partial \dot{R}/\partial \underline{x}$ are clearly the same as before, but

$$\partial(\Delta R_i)/\partial \underline{x} = \frac{1}{R(R-\Delta R_i)} \Big[\Big[(x-x_s)(R-\Delta R_i) - (x-x_{si})R \Big] ,$$

$$\Big[(y-y_s)(R-\Delta R_i) - (y-y_{si})R \Big] ,$$

$$\Big[(z-z_s)(R-\Delta R_i) - (z-z_{si})R \Big] ,$$

$$0, 0, 0 \Big] ,$$

$$\partial(\Delta \dot{R}_i)/\partial \underline{x} = \Big[\Big[\frac{R(\dot{x}+\omega_e y_s) - \dot{R}(x-x_s)}{R^2} - \frac{\dot{x}+\omega_e y_{si}}{R-\Delta R_i} + \frac{(\dot{R}-\Delta\dot{R}_i)(x-x_{si})}{(R-\Delta R_i)^2} \Big] ,$$

$$\Big[\frac{R(\dot{y}-\omega_e x_s) - \dot{R}(y-y_s)}{R^2} - \frac{\dot{y}-\omega_e x_{si}}{R-\Delta R_i} + \frac{(\dot{R}-\Delta\dot{R}_i)(x-x_{si})}{(R-\Delta R_i)^2} \Big] ,$$

$$\Big[\frac{R\dot{z} - \dot{R}(z-z_s)}{R^2} - \frac{\dot{z}}{R-\Delta R_i} + \frac{(\dot{R}-\Delta\dot{R}_i)(z-z_{si})}{(R-\Delta R_i)^2} \Big] ,$$

$$\Big[\frac{x-x_s}{R} - \frac{x-x_{si}}{R-\Delta R_i} \Big] , \Big[\frac{y-y_s}{R} - \frac{y-y_{si}}{R-\Delta R_i} \Big] , \Big[\frac{z-z_s}{R} - \frac{z-z_{si}}{R-\Delta R_i} \Big] \Big] \qquad \text{(III.12)}$$

$i = 1,2.$

These are row entries in

$$H = \begin{bmatrix} \partial R/\partial \underline{x} \\ \partial(\Delta R_1)/\partial \underline{x} \\ \partial(\Delta R_2)/\partial \underline{x} \\ \partial \dot{R}/\partial \underline{x} \\ \partial(\Delta \dot{R}_1)/\partial \underline{x} \\ \partial(\Delta \dot{R}_2)/\partial \underline{x} \end{bmatrix}$$

The noise matrix H_η is now a 6 x 6 identity matrix, and the bias matrix H_b is the 6 x 16 matrix

$$H_b = \left[\begin{array}{c|c|c|c|c} I & \dfrac{\partial \underline{h}}{\partial \underline{r}_s}\, T(t) & \dfrac{\partial \underline{h}}{\partial \Delta \underline{r}_{s1}}\, T(t) & \dfrac{\partial \underline{h}}{\partial \Delta \underline{r}_{s2}}\, T(t) & \dfrac{\partial \underline{h}}{\partial t} \end{array}\right], \qquad \text{(III.14)}$$

where

$$\frac{\partial \underline{h}}{\partial \underline{r}_s} = \begin{bmatrix} \partial R/\partial \underline{r}_s \\ \partial(\Delta R_1)/\partial \underline{r}_s \\ \partial(\Delta R_2)/\partial \underline{r}_s \\ \partial \dot{R}/\partial \underline{r}_s \\ \partial(\Delta \dot{R}_1)/\partial \underline{r}_s \\ \partial(\Delta \dot{R}_2)/\partial \underline{r}_s \end{bmatrix},$$

$$\frac{\partial \underline{h}}{\partial \Delta \underline{r}_{s1}} = \begin{bmatrix} 0 \\ \partial(\Delta R_1)/\partial \Delta \underline{r}_{s1} \\ 0 \\ 0 \\ \partial(\Delta \dot{R}_1)/\partial \Delta \underline{r}_{s1} \\ 0 \end{bmatrix},$$

$$\frac{\partial \underline{h}}{\partial \Delta \underline{r}_{s2}} = \begin{bmatrix} 0 \\ 0 \\ \partial(\Delta R_2)/\partial \Delta \underline{r}_{s2} \\ 0 \\ 0 \\ \partial(\Delta \dot{R}_2)/\partial \Delta \underline{r}_{s2} \end{bmatrix},$$

$$\frac{\partial \underline{h}}{\partial t} = \begin{bmatrix} \partial R/\partial t \\ \partial(\Delta R_1)/\partial t \\ \partial(\Delta R_2)/\partial t \\ \partial \dot{R}/\partial t \\ \partial(\Delta \dot{R}_1)/\partial t \\ \partial(\Delta \dot{R}_2)/\partial t \end{bmatrix} .$$

Now, the surveys for the three stations are such that the master station at $\underline{r}_s$ is located by geodetic survey. Its position has survey biases in the earth-fixed system (X^1, Y^1, Z^1). The slave stations are surveyed relative to the master:

$$\underline{r}_{si} = \underline{r}_s + \Delta\underline{r}_{si} , \quad i = 1, 2, \tag{III.15}$$

with the relative biases on the relative position vectors $\Delta\underline{r}_{si}$ independent of and much smaller than the absolute survey bias on the master station.

The bias vector is the 16 x 1 array

$$\underline{b} = \begin{Bmatrix} R & \text{Range Bias} \\ \Delta R_1 & \text{Range Bias} \\ \Delta R_2 & \text{Range Bias} \\ \dot{R} & \text{Range-Rate Bias} \\ \Delta \dot{R}_1 & \text{Range-Rate Bias} \\ \Delta \dot{R}_2 & \text{Range-Rate Bias} \\ x^1 & \text{Master Station Location Bias} \\ y^1 & \text{Master Station Location Bias} \\ z^1 & \text{Master Station Location Bias} \\ \Delta x^1 & \text{Slave 1 Relative Location Bias} \\ \Delta y^1 & \text{Slave 1 Relative Location Bias} \end{Bmatrix}$$

$$\left\{\begin{array}{ll} \Delta z^1 & \text{Slave 1 Relative Location Bias} \\ \Delta x^1 & \text{Slave 2 Relative Location Bias} \\ \Delta y^1 & \text{Slave 2 Relative Location Bias} \\ \Delta z^1 & \text{Slave 2 Relative Location Bias} \\ \text{Clock Bias} & \end{array}\right\}$$

Upon putting (III.15) into (III.11), defining

$$\begin{aligned} R_i &= R-\Delta R_i, \\ \dot{R}_i &= \dot{R}-\Delta\dot{R}_i, \end{aligned} \tag{III.16}$$

and taking derivatives, we find, for the range variables,

$$\begin{aligned} \partial R/\partial \underline{r}_s &= -\partial R/\partial \underline{r} \quad , \\ \partial(\Delta R_i)/\partial \underline{r}_s &= \partial R/\partial \underline{r}_s + \partial(\Delta R_i)/\partial(\Delta \underline{r}_{si}) \quad , \\ \partial(\Delta R_i)/\partial(\Delta \underline{r}_{si}) &= (1/R_i)\left[(x-x_{si}) \ , \ (y-y_{si}) \ , \ (z-z_{si})\right] \quad , \end{aligned} \tag{III.17}$$

where the second equation results from expanding ΔR_i into $R-R_i$ and noting that $-\partial R_i/\partial \underline{r}_s = \partial(\Delta R_i)/\partial(\Delta \underline{r}_{si})$. For the range rates,

$$\begin{aligned} \partial \dot{R}/\partial \underline{r}_s &= \text{as given in (III.8)} \ , \\ \partial(\Delta \dot{R}_i)/\partial \underline{r}_s &= \partial \dot{R}/\partial \underline{r}_s + \partial(\Delta \dot{R}_i)/\partial(\Delta \underline{r}_{si}) \\ \partial(\Delta \dot{R}_i)/\partial(\Delta \underline{r}_{si}) &= \frac{1}{R_i^2}\Big[\left[R_i(\dot{x}+\omega_e y) - \dot{R}_i(x-x_{si})\right], \\ &\qquad \left[R_i(\dot{y}-\omega_e x) - \dot{R}_i(y-y_{si})\right], \\ &\qquad \left[R_i \dot{z} - \dot{R}_i(z-z_{si})\right] \Big] \end{aligned} \tag{III.18}$$

The time derivatives for $\partial \underline{h}/\partial t$ are

$$\partial \dot{R}/\partial t = (\partial R/\partial \underline{r})\ \dot{\underline{r}} + (\partial R/\partial \underline{r}_s)\ \dot{\underline{r}}_s \quad ,$$

$$\partial(\Delta \dot{R}_i)/\partial t = [\partial(\Delta R_i)/\partial \underline{r}]\ \dot{\underline{r}} + [\partial(\Delta R_i)/\partial \underline{r}_s]\ \dot{\underline{r}}_s + [\partial(\Delta R_i)/\partial(\Delta \underline{r}_{si})]\ \Delta \dot{\underline{r}}_{si} \quad ,$$

$$\partial \dot{\hat{R}}/\partial t = (\partial \dot{\hat{R}}/\partial \underline{x})\ \dot{\underline{x}} + (\partial \dot{\hat{R}}/\partial \underline{r}_s)\ \dot{\underline{r}}_s \quad ,$$

$$\partial(\Delta \dot{\hat{R}}_i)/\partial t = [\partial(\Delta \dot{\hat{R}}_i)/\partial \underline{x}]\ \dot{\underline{x}} + [\partial(\Delta \dot{\hat{R}}_i)/\partial \underline{r}_s]\ \dot{\underline{r}}_s + [\partial(\Delta \dot{\hat{R}}_i)/\partial(\Delta \underline{r}_{si})]\ \Delta \dot{\underline{r}}_{si} \qquad \text{(III.19)}$$

C. BAKER-NUNN CAMERAS

The Baker-Nunn cameras record right ascension and declination of the target. These are, respectively,

$$\alpha = \tan^{-1}\left(\frac{y-y_s}{x-x_s}\right) - \gamma$$

$$\delta = \sin^{-1}\left(\frac{z-z_s}{R}\right) \quad , \qquad \text{(III.20)}$$

where γ is the right ascension of Greenwich, the "Greenwich Hour Angle."

The observation vector is

$$\underline{z} = \begin{bmatrix} \alpha \\ \delta \end{bmatrix} = \underline{h}\ (\underline{x},\ \eta,\ \underline{b},\ t).$$

The partial derivatives are as follows:

$$\partial \alpha / \partial \underline{x} = \frac{1}{\sec^2 \alpha} \left[\frac{y-y_s}{(x-x_s)^2} \ , \ \frac{1}{x-x_s} \ , \ 0,\ 0,\ 0,\ 0 \right],$$

$$\partial \delta / \partial \underline{x} = \frac{-(z-z_s)}{R^3 \cos \delta} \left[(x-x_s) \ , \ (y-y_s) \ , \ \frac{(z-z_s)^2 - R^2}{(z-z_s)} \ , \ 0,\ 0,\ 0 \right],$$

for

$$H = \begin{bmatrix} \partial \alpha / \partial \underline{x} \\ \partial \delta / \partial \underline{x} \end{bmatrix} . \qquad \text{(III.22)}$$

The noise matrix, since a fluctuating time error is assumed for this case, is now the 2 x 3 array

$$H_\eta = \left[\begin{array}{cc|c} 1 & 0 & \partial \alpha / \partial t \\ 0 & 1 & \partial \delta / \partial t \end{array}\right] , \qquad \text{(III.23)}$$

where

$$-\partial \alpha / \partial \underline{r}_s = \partial \alpha / \partial \underline{r} \ ,$$

$$-\partial \delta / \partial \underline{r}_s = \partial \delta / \partial \underline{r} \ ,$$

and

$$\partial \alpha / \partial t = (\partial \alpha / \partial \underline{r})\ \dot{\underline{r}} + (\partial \alpha / \partial \underline{r}_s)\ \dot{\underline{r}}_s - \partial \gamma / \partial t$$

$$\partial \delta / \partial t = (\partial \delta / \partial \underline{r})\ \dot{\underline{r}} + (\partial \delta / \partial \underline{r}_s)\ \dot{\underline{r}}_s \ , \qquad \text{(III.24)}$$

where, to a high degree of accuracy for orbital durations on the order of years, $\partial \gamma / \partial t = \omega_e = \text{const.}$ These are also used in the 2 x 6 matrix

$$H_b = \left[\begin{array}{cc|c|c} 1 & 0 & \dfrac{\partial \underline{h}}{\partial \underline{r}_s}\ T(t) & \partial \alpha / \partial t \\ 0 & 1 & & \partial \delta / \partial t \end{array}\right], \qquad \text{(III.25)}$$

which corresponds to the bias vector

$$\underline{b} = \begin{bmatrix} \text{Right Ascension Bias} \\ \text{Declination Bias} \\ x^1 \text{ Station Location Bias} \\ y^1 \text{ Station Location Bias} \\ z^1 \text{ Station Location Bias} \\ \text{Clock Bias} \end{bmatrix}$$

UNCLASSIFIED

Security Classification

DOCUMENT CONTROL DATA - R&D

(Security classification of title, body of abstract and indexing annotation must be entered when the overall report is classified)

1. ORIGINATING ACTIVITY *(Corporate author)*

Westinghouse Defense and Space Center
Surface Division
Baltimore, Maryland

2a. REPORT SECURITY CLASSIFICATION

UNCLASSIFIED

2b GROUP

N/A

3. REPORT TITLE

MODELS FOR ANALYSIS OF THE CAPABILITIES OF GROUND BASED SENSORS IN DETERMINING THE MASS OF ORBITING BODIES- EXTENDED MODELS

4. DESCRIPTIVE NOTES *(Type of report and inclusive dates)*

Technical Report Number 3 (Task II)

5. AUTHOR(S) *(Last name, first name, initial)*

Culver, Walter J. - Doeg, Donald S.; Gilbert, Willard L.; Marquart, R. Gary

6. REPORT DATE	7a. TOTAL NO. OF PAGES	7b. NO. OF REFS
August 1967	60	5

8a. CONTRACT OR GRANT NO.	9a. ORIGINATOR'S REPORT NUMBER(S)
F19628-67-C0041	
b. PROJECT NO.	ESD-TR-68-157, Vol. II
c.	9b. OTHER REPORT NO(S) *(Any other numbers that may be assigned this report)*
d.	

10. AVAILABILITY/LIMITATION NOTICES

This document has been approved for public release and sale; its distribution is unlimited.

11. SUPPLEMENTARY NOTES	12. SPONSORING MILITARY ACTIVITY
	Space Defense Systems Program Office, Electronic Systems Division, Air Force Systems Command, USAF, L.G. Hanscom Fld, Bedford, Mass. 01730

13. ABSTRACT

This report contains a description of the models to be used in analyzing the capabilities of ground-based sensors in determining the mass of orbiting bodies, model coefficients, and the justification for their selection. Relations are derived for computing sensitivity coefficients and their coupling to mass variance for the case of noisy, biased sensors (monostatic and tri-static radars, Baker - Nunn cameras), and for spherical and tumbling cylindrical satellites.

DD FORM 1 JAN 64 1473

UNCLASSIFIED

Security Classification

UNCLASSIFIED

Security Classification

14 KEY WORDS	LINK A		LINK B		LINK C	
	ROLE	WT	ROLE	WT	ROLE	WT
RADAR MASS ERRORS ANALYSIS SENSOR ORBIT SATELLITE						

INSTRUCTIONS

1. ORIGINATING ACTIVITY: Enter the name and address of the contractor, subcontractor, grantee, Department of Defense activity or other organization *(corporate author)* issuing the report.

2a. REPORT SECURITY CLASSIFICATION: Enter the overall security classification of the report. Indicate whether "Restricted Data" is included. Marking is to be in accordance with appropriate security regulations.

2b. GROUP: Automatic downgrading is specified in DoD Directive 5200.10 and Armed Forces Industrial Manual. Enter the group number. Also, when applicable, show that optional markings have been used for Group 3 and Group 4 as authorized.

3. REPORT TITLE: Enter the complete report title in all capital letters. Titles in all cases should be unclassified. If a meaningful title cannot be selected without classification, show title classification in all capitals in parenthesis immediately following the title.

4. DESCRIPTIVE NOTES: If appropriate, enter the type of report, e.g., interim, progress, summary, annual, or final. Give the inclusive dates when a specific reporting period is covered.

5. AUTHOR(S): Enter the name(s) of author(s) as shown on or in the report. Enter last name, first name, middle initial. If military, show rank and branch of service. The name of the principal author is an absolute minimum requirement.

6. REPORT DATE: Enter the date of the report as day, month, year; or month, year. If more than one date appears on the report, use date of publication.

7a. TOTAL NUMBER OF PAGES: The total page count should follow normal pagination procedures, i.e., enter the number of pages containing information.

7b. NUMBER OF REFERENCES: Enter the total number of references cited in the report.

8a. CONTRACT OR GRANT NUMBER: If appropriate, enter the applicable number of the contract or grant under which the report was written.

8b, 8c, & 8d. PROJECT NUMBER: Enter the appropriate military department identification, such as project number, subproject number, system numbers, task number, etc.

9a. ORIGINATOR'S REPORT NUMBER(S): Enter the official report number by which the document will be identified and controlled by the originating activity. This number must be unique to this report.

9b. OTHER REPORT NUMBER(S): If the report has been assigned any other report numbers *(either by the originator or by the sponsor)*, also enter this number(s).

10. AVAILABILITY/LIMITATION NOTICES: Enter any limitations on further dissemination of the report, other than those imposed by security classification, using standard statements such as:

(1) "Qualified requesters may obtain copies of this report from DDC."

(2) "Foreign announcement and dissemination of this report by DDC is not authorized."

(3) "U. S. Government agencies may obtain copies of this report directly from DDC. Other qualified DDC users shall request through

_____."

(4) "U. S. military agencies may obtain copies of this report directly from DDC. Other qualified users shall request through

_____."

(5) "All distribution of this report is controlled. Qualified DDC users shall request through

_____."

If the report has been furnished to the Office of Technical Services, Department of Commerce, for sale to the public, indicate this fact and enter the price, if known.

11. SUPPLEMENTARY NOTES: Use for additional explanatory notes.

12. SPONSORING MILITARY ACTIVITY: Enter the name of the departmental project office or laboratory sponsoring *(paying for)* the research and development. Include address.

13. ABSTRACT: Enter an abstract giving a brief and factual summary of the document indicative of the report, even though it may also appear elsewhere in the body of the technical report. If additional space is required, a continuation sheet shall be attached.

It is highly desirable that the abstract of classified reports be unclassified. Each paragraph of the abstract shall end with an indication of the military security classification of the information in the paragraph, represented as *(TS)*, *(S)*, *(C)*, or *(U)*.

There is no limitation on the length of the abstract. However, the suggested length is from 150 to 225 words.

14. KEY WORDS: Key words are technically meaningful terms or short phrases that characterize a report and may be used as index entries for cataloging the report. Key words must be selected so that no security classification is required. Identifiers, such as equipment model designation, trade name, military project code name, geographic location, may be used as key words but will be followed by an indication of technical context. The assignment of links, roles, and weights is optional.

DD FORM 1 JAN 64 1473 (BACK)

UNCLASSIFIED

Security Classification